



저작자표시-비영리-변경금지 2.0 대한민국

이용자는 아래의 조건을 따르는 경우에 한하여 자유롭게

- 이 저작물을 복제, 배포, 전송, 전시, 공연 및 방송할 수 있습니다.

다음과 같은 조건을 따라야 합니다:



저작자표시. 귀하는 원저작자를 표시하여야 합니다.



비영리. 귀하는 이 저작물을 영리 목적으로 이용할 수 없습니다.



변경금지. 귀하는 이 저작물을 개작, 변형 또는 가공할 수 없습니다.

- 귀하는, 이 저작물의 재이용이나 배포의 경우, 이 저작물에 적용된 이용허락조건을 명확하게 나타내어야 합니다.
- 저작권자로부터 별도의 허가를 받으면 이러한 조건들은 적용되지 않습니다.

저작권법에 따른 이용자의 권리는 위의 내용에 의하여 영향을 받지 않습니다.

이것은 [이용허락규약\(Legal Code\)](#)을 이해하기 쉽게 요약한 것입니다.

[Disclaimer](#)

Optimal Nesting and Generation of Cutting
Paths for Model Ship Production

2023 08

심사위원 신 동 목 인

심사위원 오 민 재 인

심사위원 김 기 수 인

2

(Nesting)

Phi-function

Breadth-first Search

(f_y, f_{xy})

(0,0)

가

가

x

y

가

가

가 가

(Polyline)

, Non-Fit-Polygon,

Optimal Nesting and Generation of Cutting Paths for Model Ship Production

Junho Choi

Department of Naval Architecture and Ocean Engineering, Ulsan University

Abstract

2D nesting, a widely employed technique in industries such as shipbuilding, automotive, and apparel, aims to minimize resource and material waste by effectively arranging components. By automating the layout process, it reduces labor and increases productivity. However, the current manual approach to piece placement in model ship production results in lengthy work hours and difficulty in finding the optimal placement with minimal material waste. To address this challenge, this study proposes an automated method for optimizing nesting in model ship production to minimize material scrap. The objective is to achieve an optimal arrangement within the raw material sheet, maximizing the number of pieces while avoiding overlapping shapes. A nesting algorithm for multiple sheet layouts, considering the characteristics of model ship pieces, is implemented. The chosen representation method is grid-based, as it provides a simple depiction of shapes and facilitates overlap detection compared to alternative methods. Additionally, a novel approach utilizing the properties of negative functions is presented to represent piece outlines on the grid. The interior of shapes is defined using the Breadth-first Search algorithm on a multidimensional array. Rotation of shapes is performed based on a global coordinate system, with adjustments made to ensure positive or zero coordinate values. The placement algorithm utilizes two objective functions to compare results, employing genetic algorithms to determine the optimal placement order that minimizes scrap rate and identify the optimal rotation angle for each piece in that order. Furthermore, a cutting path generation algorithm is introduced to minimize tool cutting paths, employing a selection process based on proximity to the origin and previously cut pieces. The algorithm calculates the minimum travel distance between points using line segments and arcs associated with each piece. The proposed method offers shorter execution times and provides reasonable cutting paths compared to metaheuristic algorithms.

목차

제1장 서론	1
1.1. 연구배경	1
1.2. 관련 연구	2
1.3. 연구 목적	3
1.4. 논문의 구성	4
제2장 형상의 표현	5
2.1. 배경 이론	5
2.2. 격자 데이터 생성 과정	6
2.3. 해상도의 정의	8
2.4. 입력 데이터	9
2.5. 피스의 외형선 정의	9
2.5.1. Implicit functions	10
2.5.1.1. Line	12
2.5.1.2. Arc	17
2.6. 피스 내부 정의 알고리즘	20
2.7. 피스의 회전	23
제3장 배치 알고리즘	25
3.1. 단일 판(single plate) 배치	25
3.2. 다중 판(multiple plate) 배치	25
3.3. 배치 순서의 결정	26

3.3.1. 유전 알고리즘	26
3.3.1.1. Fitness function	28
3.3.1.2. Selection	30
3.3.1.3. Crossover	30
3.3.1.4. Mutation	31
3.4. 피스의 배치	33
3.4.1. 배치 알고리즘	33
3.4.2. 목적함수	35
3.5. 배치 결과	37
제4장 절단 경로 생성	42
4.1 G-code	42
4.2 피스의 절단 순서 결정	44
4.2.2 절단 경로 알고리즘	48
4.2.3 실제 모형선 피스에 대한 절단 경로 생성 알고리즘 검증	51
제5장 결론 및 고찰	52

표 목차

Table. 2.1. Determining the sign of the equation of a straight line	11
Table. 2.2. Determining the sign of the equation of an arc	12
Table. 2.3. Range of α and β to represent an arc	17
Table. 3.1. The procedure of a general GA[30]	28
Table. 4.1. G-code list	42
Table. 4.2. Determination of convexity according to arc angle	47

그림 목차

Fig. 1.1. Model ship manufacturing process	1
Fig. 2.1. No-Fit-Polygon method	5
Fig. 2.2. Grid representation method	5
Fig. 2.3. Algorithm flow chart for model ship piece placement and cutting path generation	6
Fig. 2.4. The process of defining the shape of a piece	7
Fig. 2.5. Placement result due to resolution difference	8
Fig. 2.6. Data of the piece shape	9
Fig. 2.7. Representation of Explicit functions and Implicit functions	10
Fig. 2.8. Expression of the implicit function for the equation of a straight line	10
Fig. 2.9. Expression of the implicit function for the equation of an arc	11
Fig. 2.10. Creation of a grid for representing line segments	13
Fig. 2. 11. Assigned values for lattice vertices	14
Fig. 2.12. Assigned values for the grid	15
Fig. 2.13. Calculation range of the grid	16
Fig. 2.14. Calculation result of the line segment	16
Fig. 2.15. and in the first quadrant	18
Fig. 2.16. Calculation range when and are in the first quadrant	18
Fig. 2.17. in the first quadrant and in the second quadrant	19
Fig. 2.18. Calculation range when is in the second quadrant and is in the second quadrant	20
Fig. 2.19. Search direction of BFS algorithm	20
Fig. 2.20. Creation of additional grids	21
Fig. 2.21. Process of BFS Algorithm	21

Fig. 2.22. Post-processing after applying the BFS algorithm	22
Fig. 2.23. Result of geometric representation of the model ship piece	22
Fig. 2.24. Arrangement at angles that cannot be placed	23
Fig. 2.25. Rotation of the piece	24
Fig. 3.1. Placing a piece on a single plate	25
Fig. 3.2. Representation of multiplate grids	26
Fig. 3.3. The components of a poluation	26
Fig. 3.4. Basic steps of genetic algorithm	27
Fig. 3.5. Case1 : Calculation of the fitness function	29
Fig. 3.6. Case2 : Calculation of the fitness function	30
Fig. 3.7. Duplication of genes	31
Fig. 3.8. Elimination of gene duplication	31
Fig. 3.9. Increased piece vertical size due to rotation of angle	32
Fig. 3.10. Mutation operation on layout order	32
Fig. 3.11. Layout algorithm flow chart	33
Fig. 3.12. Overlap detection of two pieces	34
Fig. 3.13. Search Range of pieces to be placed	35
Fig. 3.14. Calculation of the objective function , , and	36
Fig. 3.15. Pieces of the Model ship	37
Fig. 3.16. Arrangement in order of aspect ratio	38
Fig. 3.17. Arrangement in order of area	38
Fig. 3.18. Case 1 of Arrangement using genetic algorithm	38
Fig. 3.19. Case 1 of Arrangement using genetic algorithm when the grid size is 50mm	39
Fig. 3.20. Case 2 of Arrangement using genetic algorithm when the grid size is 25mm	39
Fig. 3.21. Case 2 of Arrangement using genetic algorithm when the grid size is 50mm	39

Fig. 3.22. Case 3 of Arrangement using genetic algorithm when the grid size is 25mm	40
Fig. 3.23. Case 3 of Arrangement using genetic algorithm when the grid size is 25mm	40
Fig. 3.24. Comparison of reusability when grid sizes are different	41
Fig. 4.1. Example for G00 and G01	42
Fig. 4.2. Example for G02 and G03	43
Fig. 4.3. Examples of reasons for judging convexity	44
Fig. 4.4. Example when the arc of the piece is convex	45
Fig. 4.5. Example when the arc of the piece is concave	46
Fig. 4.6. Exception Case example when the arc of the piece is concave	46
Fig. 4.7. Exception case example when the arc of the piece is convex	47
Fig. 4.8. Example of arrangement result including arc and line	48
Fig. 4.9. Example of how to select the first piece	49
Fig. 4.10. Example of how to select the second piece	49
Fig. 4.11. method for calculating the shortest path between the first piece and the second piece	50
Fig. 4.12. Result of piece cutting completion	50
Fig. 4.13. Verification of cutting path generation algorithm of model ship pieces	51

1
1.1.

가
,
가
.[1]

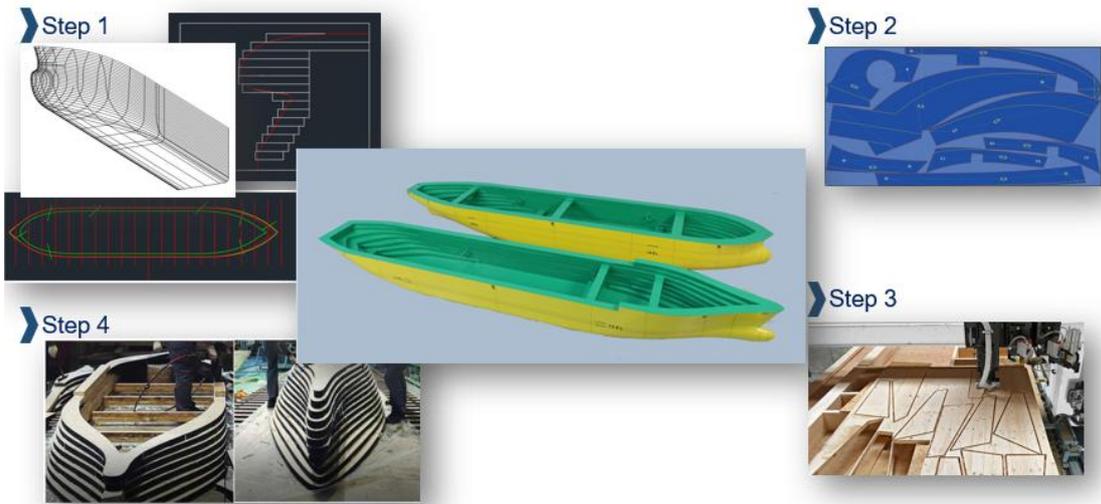


Fig. 1.1. Model ship manufacturing process

Fig. 1.1. . CAD
waterline section .
가 2400mm, 1200mm (Scrap
ratio)
NC (Numerical Control)

가
가
가
가
NC
가

NC

1.2.

[2]

. Dori, D. and Ben-Bassat[3]

. Adamowicz, M. and Albano, A.[4][5]

Non-Fit-Polygon(NFP)

. Babu

A.R and Babu N.R[6] 2

[7],

[8],

[9]

Kang[10]

. Kim[11]

Sliding

, Weng and Kuo[12] Bottom-left filling

algorithm, Tabu search Genetic algorithm, Greedy [13]

[14][15], 가 [16]

가

가 가 .[17]

NP-hard(Non-deterministic Polynomial-time
hard) 가 .[9] Park[18]
Han[9] (Piercing Point)
. Al-Sahib[19]

. Lee[20]

2 . Hajad[21]
Large

Neighborhood Search (Simulated Annealing)
. Bang[22]
. Manber and Israni[23]
. Jo[24], Han[25]

1.3.

Implicit function
'1'
[26] Breath-first Search
'1'

Kang[10]

가 , 가

가

가

가 . 가 가 . (Polygon)
(Polyline)

1.4.

, 4 . 2 5 , 3

2
2.1.

. No-Fit-Polygon(NFP)

. Fig.
NFP

2.1.

A, B가

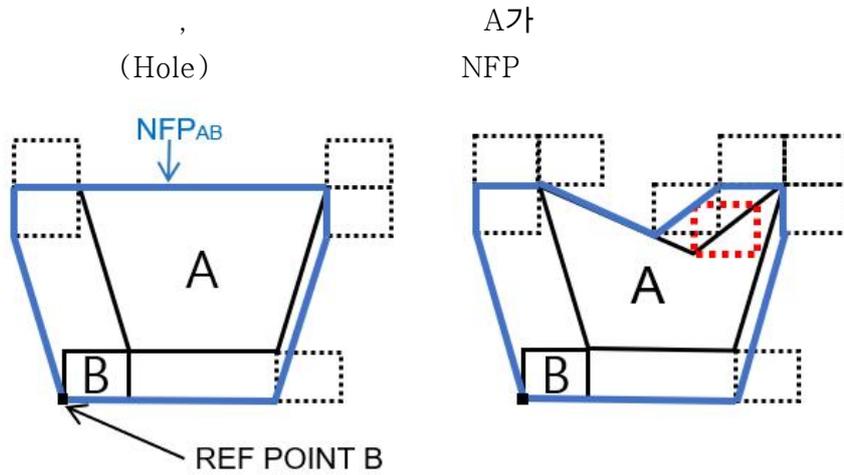


Fig. 2.1. No-Fit-Polygon method

Fig. 2.2.

. NFP

가

가

가

가

가

가

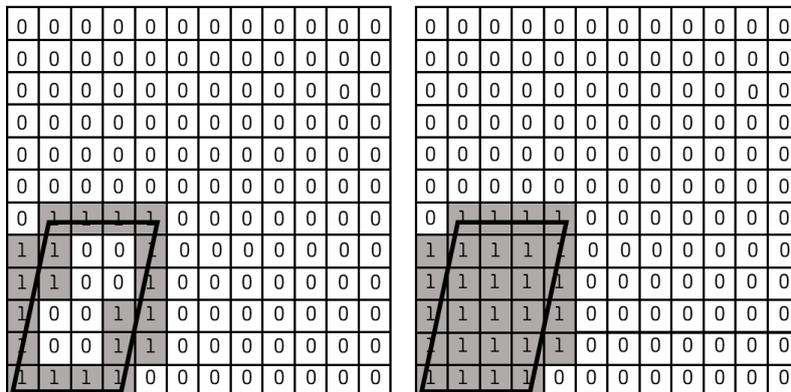


Fig. 2.2. Grid representation method

NFP

, 2

가 .[27] NFP
 .[27]
 . NFP
 가 .
 implicit function

Fig. 2.3.

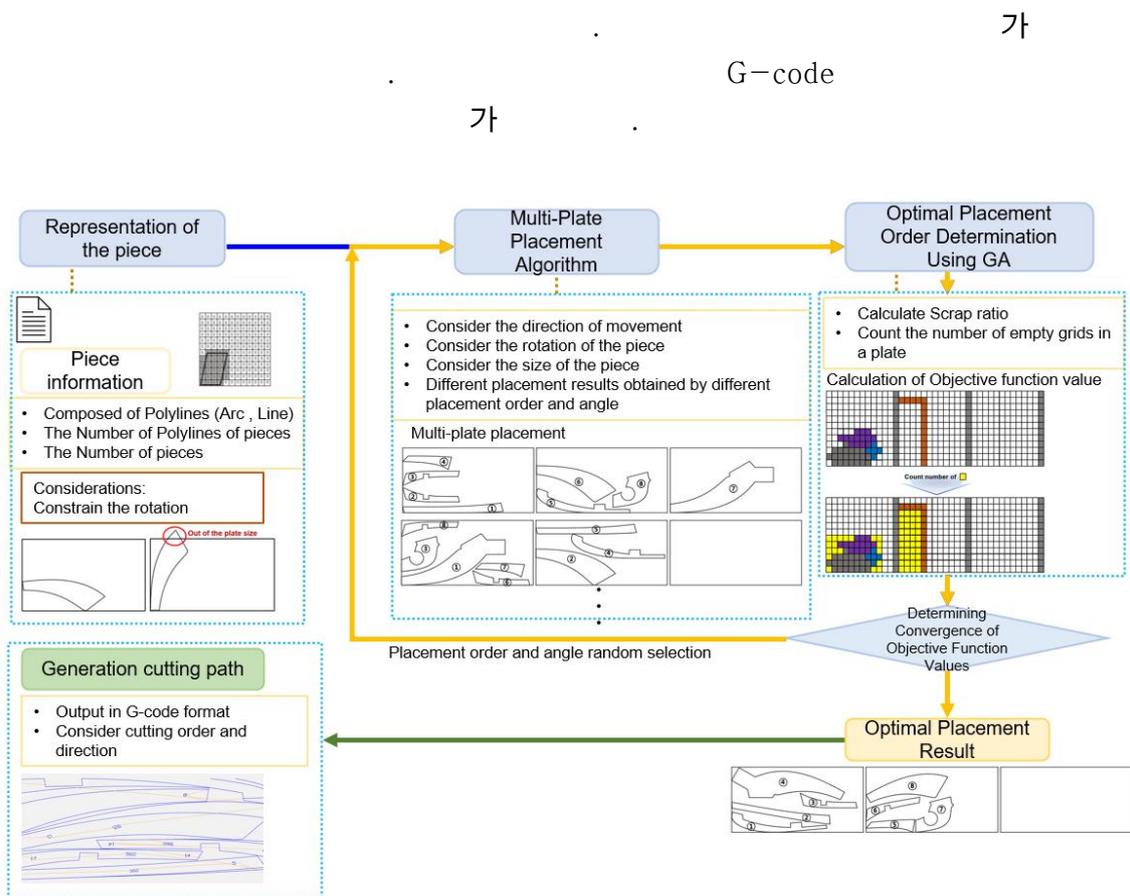


Fig. 2.3. Algorithm flow chart for model ship piece placement and cutting path generation

2.2.

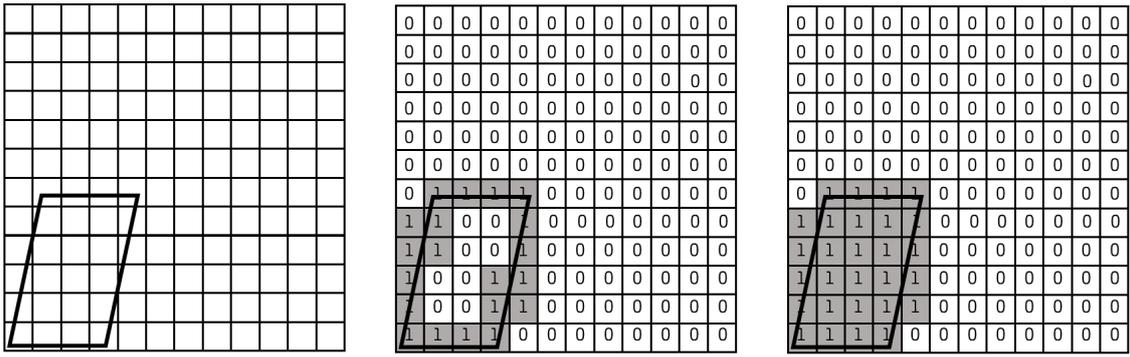


Fig. 2.4. The process of defining the shape of a piece

Fig. 2.4.

가

2

'0'

'1'

'1'

2.4.

	8					→ the Number of pieces
Piece 1	26					→ the Number of Lines of piece 1
	1					→ the Number of Arcs of piece 1
	29.031	0	0	108.342		→ The start and end points of each Line
	0	108.342	480.507	108.343		
	480.507	108.343	596.229	108.668		
	596.229	108.668	706.340	109.604		
	706.340	109.604	821.490	111.326		
		:				
		:				
		:				
	:					
	1385.762	12.348	269	271	10	→ Center point, start angle, end angle, radius of each Arc
Piece 2	23					
	7					
	59.075	220.474	0	0		
	350.38	262.461	308.434	259.165		
	394.517	264.921	350.38	262.461		
	476.131	267.629	394.517	264.921		
		:				
		:				
		:				
		433.594	-1405.1	98.85	102.97	1668.256
	480.168	-1704.2	95	98.85	1970.948	
	:					
	:					
	:					

Fig. 2.6. Data of the piece shape

CAD

Fig. 2.6.

(line) , (arc) , (start point) (end point), (center point), (start angle), (end angle), (radius) .

2.5.

2.5.1

2.5.1.1, 2.5.1.2

2.5.1. Implicit functions

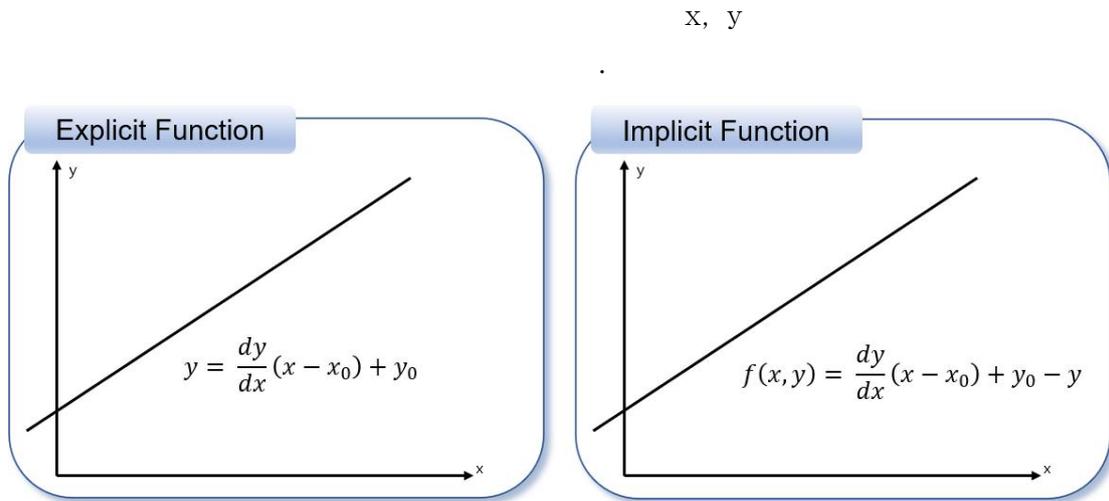


Fig. 2.7. Representation of Explicit functions and Implicit functions

Fig. 2.7.

Explicit function

$y = f(x)$

Explicit function

$f(x, y)$

Explicit function

x x

Implicit function

Explicit function

Explicit function

y

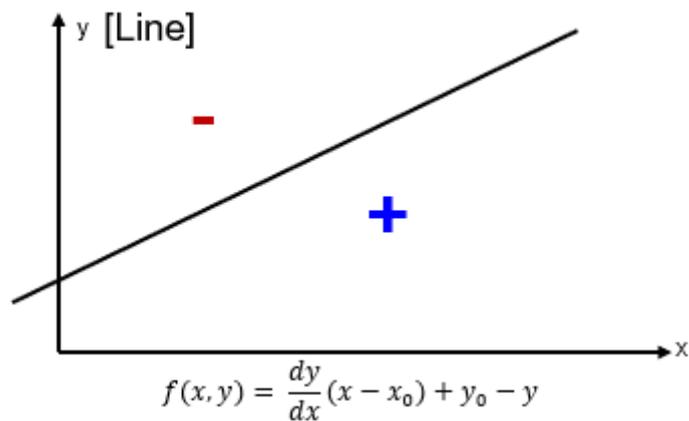


Fig. 2.8. Expression of the implicit function for the equation of a straight line

Table. 2.1. Determining the sign of the equation of a straight line

position of (x_1, y_1)	sign
upper side of the line	$f(x_1, y_1) < 0$
down side of the line	$f(x_1, y_1) > 0$
on the line	$f(x_1, y_1) = 0$

Implicit function $f(x, y) = 0$ Fig. 2.8. Table. 2.1.
 , (x_1, y_1) Implicit function ,
 '0' . (x_1, y_1)
 , 0
 . '-1', '1', '0'
 '1' 4 '0'

Fig. 2.9. Table. 2.2. Implicit function 가 θ_1 θ_2

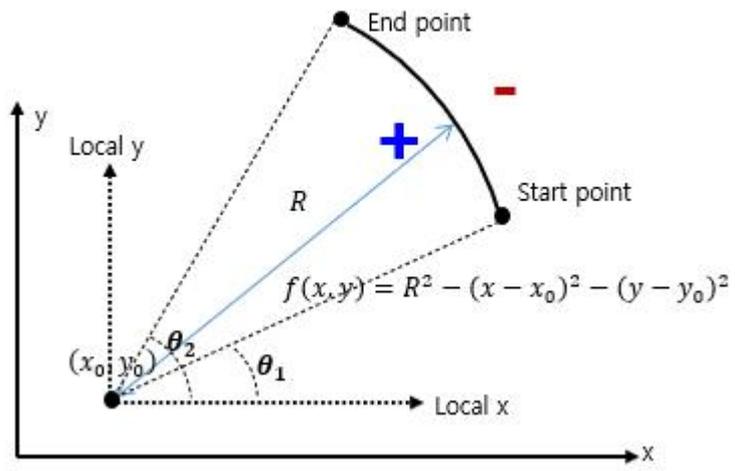


Fig. 2.9. Expression of the implicit function for the equation of an arc

Table. 2.2. Determining the sign of the equation of an arc

position of (x_1, y_1)	sign
outside of the arc	$f(x_1, y_1) < 0$
inside of the arc	$f(x_1, y_1) > 0$
on the arc	$f(x_1, y_1) = 0$

2.5.1.1. Line

Bresenham's algorithm[28]

가 1

implicit function

가

(0.5,0.5) (3.2,3.5)

explicit function (2.1)

$$y = \frac{10}{9}x - \frac{1}{18} \quad (2.1)$$

implicit function (2.2)

$$f(x,y) = \frac{10}{9}x - \frac{1}{18} - y \quad (2.2)$$

가 가 6

1 가 가 7 . (Fig. 2.10.)

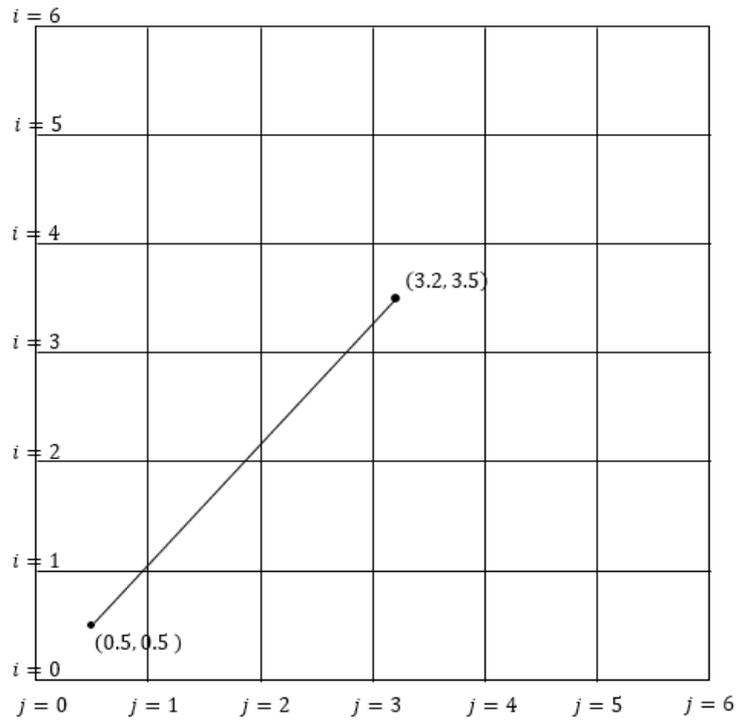


Fig. 2.10. Creation of a grid for representing line segments

(2.3) (a,b) '0' '1' , '0'
 '-1' , '0' '0' . Fig. 2.11.
 '-1' '1' .

$$\begin{aligned}
 f(a,b) > 0 & : 1 \\
 f(a,b) < 0 & : -1 \\
 f(a,b) = 0 & : 0
 \end{aligned}
 \tag{2.3}$$

'1'

'0'

Fig. 2.12.

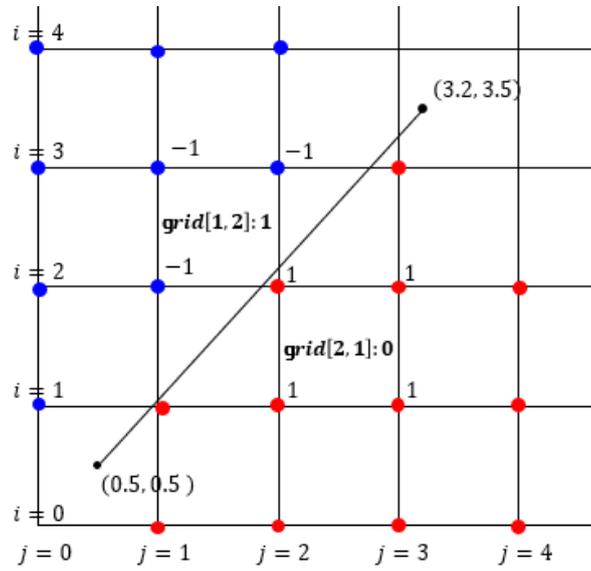


Fig. 2.12. Assigned values for the grid

$i = 1, j = 2$

가

'-2'

'1'

$i = 2, j = 1$

가

'4'

'0'

'1'

(2.5)

(2.6)

$$(\text{int})y_0 \leq i < (\text{int})y_1, (y_0 < y_1)$$

(2.5)

$$(\text{int})x_0 \leq j < (\text{int})x_1, (x_0 < x_1)$$

(2.6)

'0'

Fig. 2.13.

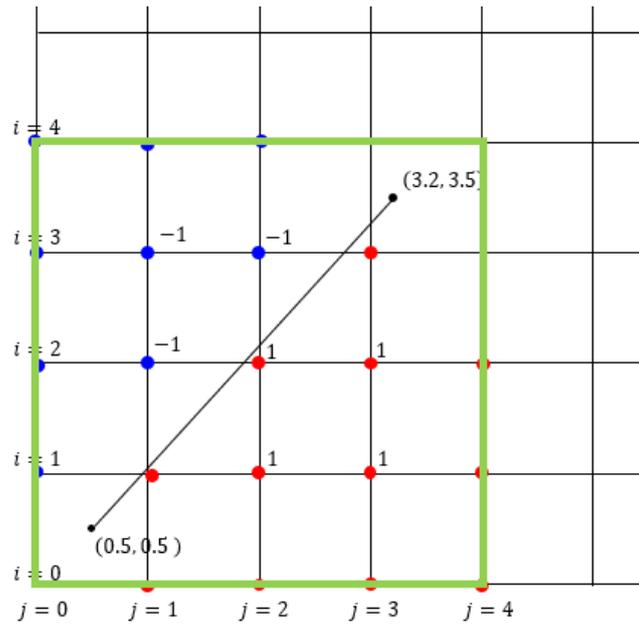


Fig. 2.13. Calculation range of the grid

Fig. 2.14. .

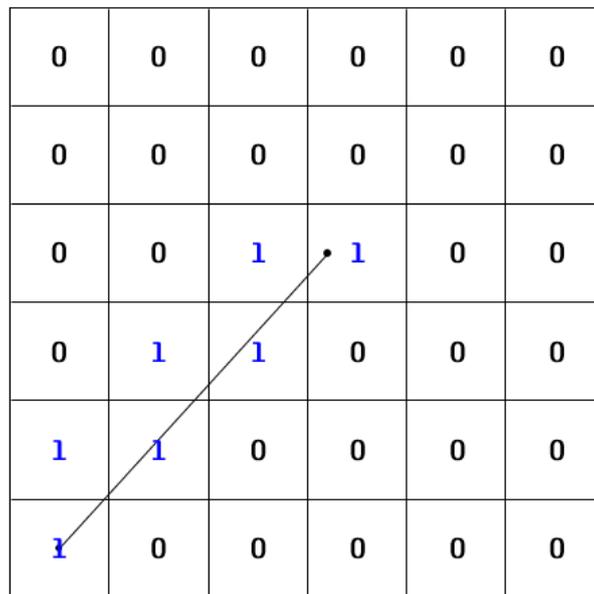


Fig. 2.14. Calculation result of the line segment

2.5.1.2. Arc

(x_0, y_0) 가 R 가 6 ,
 6 가 , 1

Table. 2.3. Range of θ_1 and θ_2 to represent an arc

θ_1	θ_2
$0^\circ \leq R < 90^\circ$	$0^\circ < R \leq 90^\circ$
	$90^\circ < R \leq 180^\circ$
	$180^\circ < R \leq 270^\circ$
	$270^\circ < R \leq 360^\circ$
$90^\circ \leq R < 180^\circ$	$90^\circ < R \leq 180^\circ$
	$180^\circ < R \leq 270^\circ$
	$270^\circ < R \leq 360^\circ$
	$360^\circ < R \leq 450^\circ$
$180^\circ \leq R < 270^\circ$	$180^\circ < R \leq 270^\circ$
	$270^\circ < R \leq 360^\circ$
	$360^\circ < R \leq 450^\circ$
	$450^\circ < R \leq 540^\circ$
$270^\circ \leq R < 360^\circ$	$270^\circ < R \leq 360^\circ$
	$360^\circ < R \leq 450^\circ$
	$450^\circ < R \leq 540^\circ$
	$540^\circ < R \leq 630^\circ$

Table. 2.3. θ_1 θ_2 가
 16가 가
 θ_1 θ_2 가
 4 가
 0

Fig. 2.15.

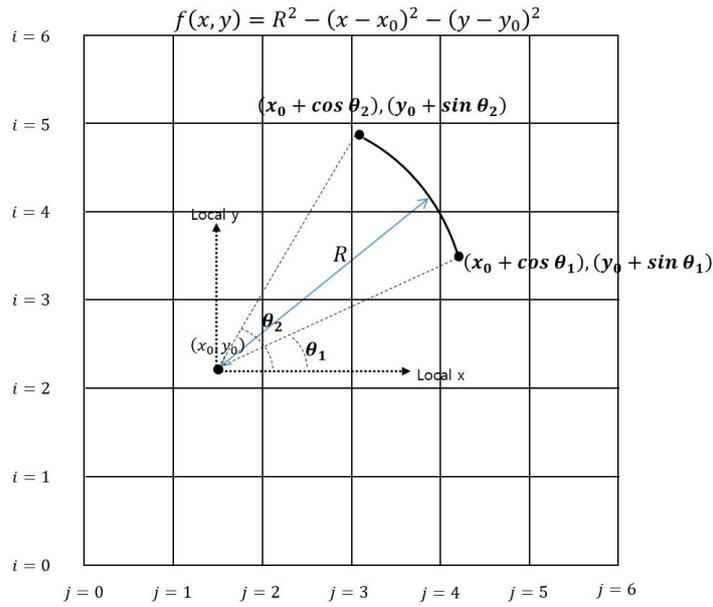


Fig. 2.15. θ_1 and θ_2 in the first quadrant

$$\theta_1 \quad \theta_2 \geq 1 \quad (2.7), \quad (2.8)$$

$$(\text{int})(y_0 + R \cdot \sin \theta_1) \leq i < (\text{int})(y_0 + R \cdot \sin \theta_2) \quad (2.7)$$

$$(\text{int})(x_0 + R \cdot \cos \theta_2) \leq j < (\text{int})(x_0 + R \cdot \cos \theta_1) \quad (2.8)$$

Fig. 2.16.

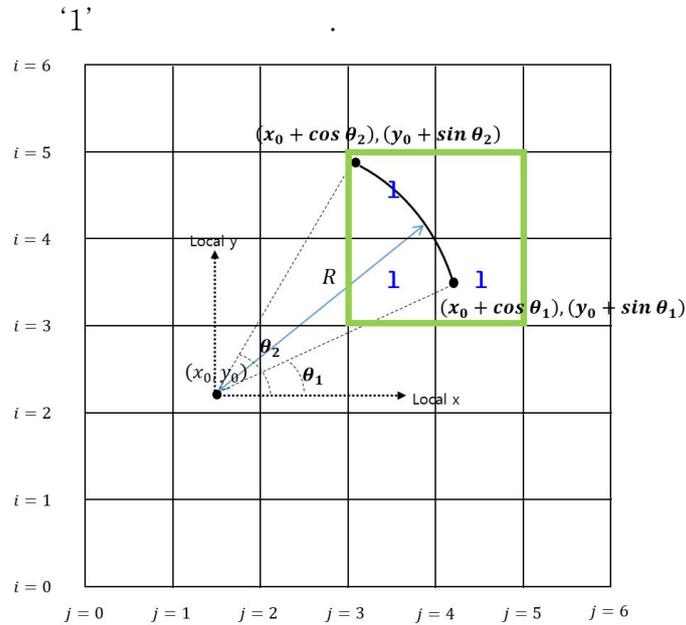


Fig. 2.16. Calculation range when θ_1 and θ_2 are in the first quadrant

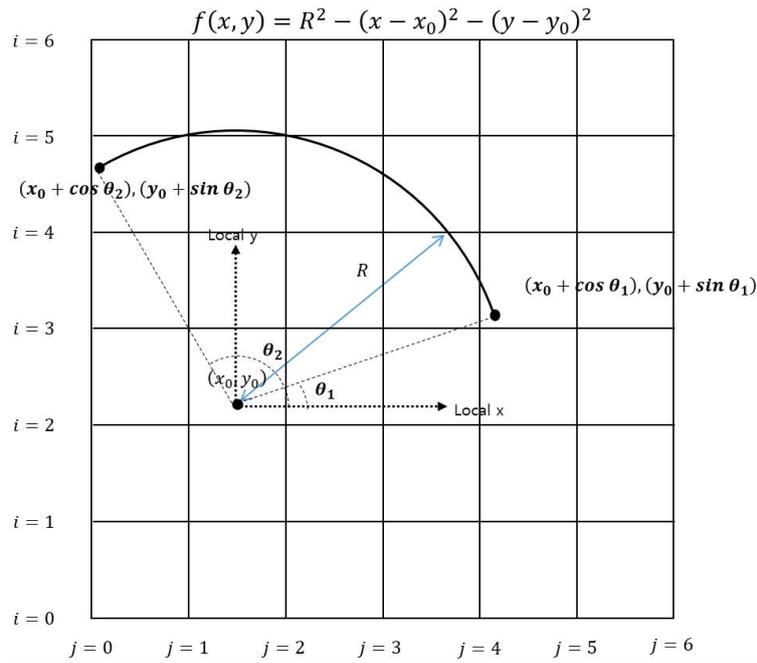


Fig. 2.17. θ_1 in the first quadrant and θ_2 in the second quadrant

Fig. 2.17.

Fig. 2.18.

2

(2.9), (2.10)

$$(\text{int})(y_0 + R \cdot \sin\theta_1) \leq i < (\text{int})(y_0 + R \cdot \sin 90^\circ) \tag{2.9}$$

$$(\text{int})(x_0 + R \cdot \cos 90^\circ) \leq j < (\text{int})(x_0 + R \cdot \cos\theta_1) \tag{2.10}$$

(2.11), (2.12)

$$(\text{int})(y_0 + R \cdot \sin\theta_2) \leq i < (\text{int})(y_0 + R \cdot \sin 90^\circ) \tag{2.11}$$

$$(\text{int})(x_0 + R \cdot \cos\theta_2) \leq j < (\text{int})(x_0 + R \cdot \cos 90^\circ) \tag{2.12}$$

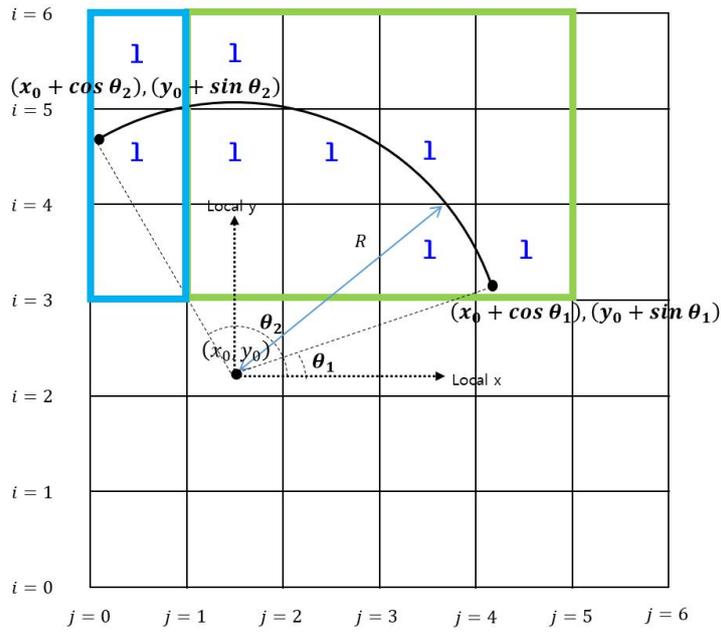


Fig. 2.18. Calculation range when θ_1 is in the second quadrant and θ_2 is in the second quadrant

2.6.

Breath-First Search(BFS)

[26] BFS

(Queue)

가 가

가

BFS

'1'

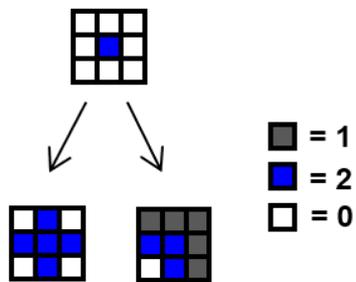


Fig. 2.19. Search direction of BFS algorithm

Fig. 2.19.

‘0’ 가 ,
 ‘2’ , BFS
 ‘0’ ‘2’
 ‘0’ ‘1’ ‘2’

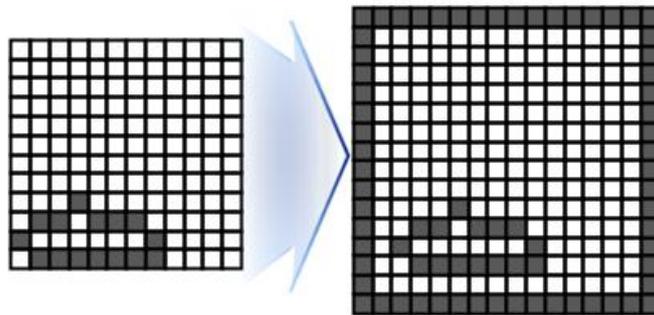


Fig. 2.20. Creation of additional grids

Fig. 2.20.

가
 ‘1’

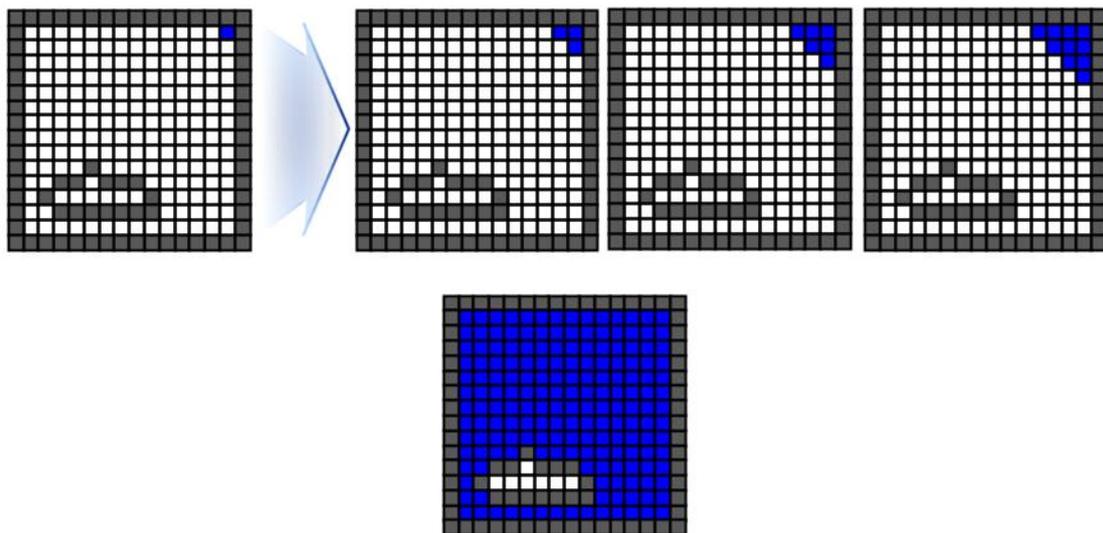


Fig. 2.21. Process of BFS Algorithm

Fig. 2.21.

	‘0’	가	가
‘2’	.	가	.

BFS

가 ‘2’

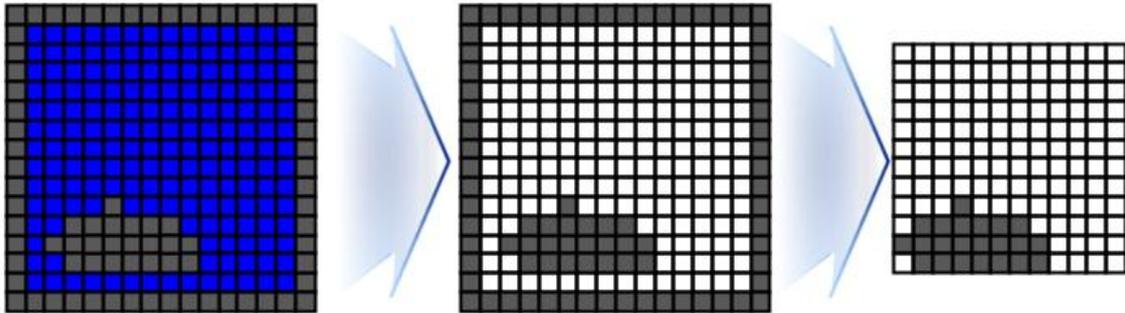


Fig. 2.22. Post-processing after applying the BFS algorithm

	가	‘2’	가		‘1’
‘2’	가		‘0’	가	.
			‘1’		.

. Fig. 2.22.

Fig. 2.23.

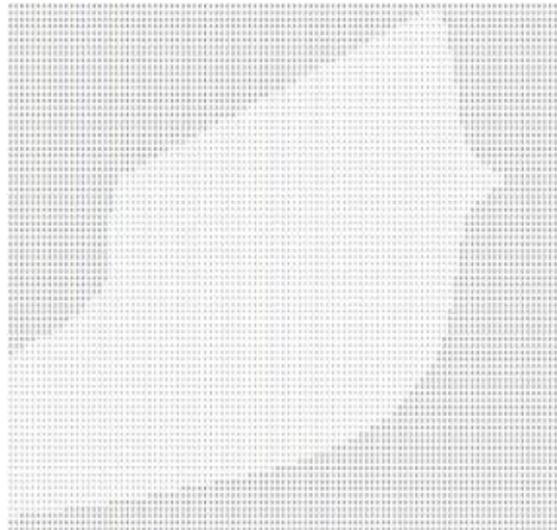


Fig. 2.23. Result of geometric representation of the model ship piece

2.7.

가
 . 0° 360°
 .
 .
 가 가
 . 가 가
 , 가
 가 가 90° 2D 가
 . 가 가
 . 0°, 5°, 10°, 15°, 20°, 30°, 60°, 90°, 120°, 150°, 180°
 °, 210°, 240°, 270°, 300°, 330°, 340°, 345°, 350°, 355°
 Fig. 2.24. 90° 가
 3 .

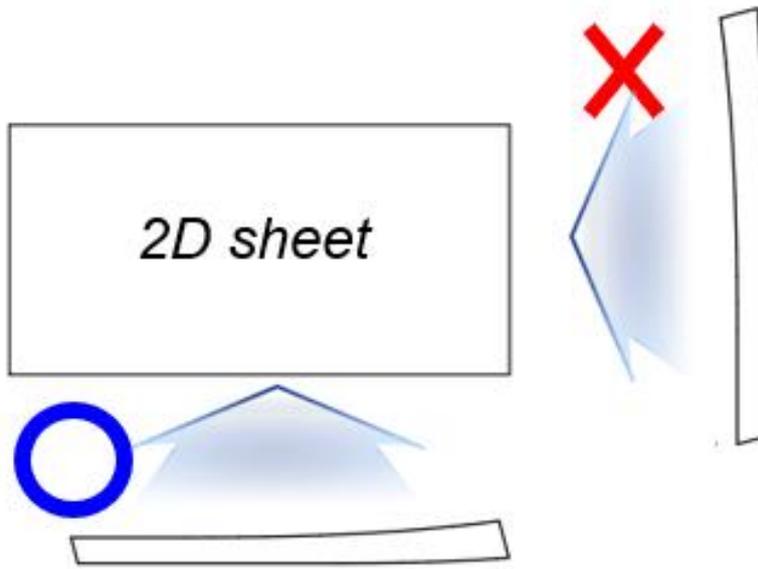


Fig. 2.24. Arrangement at angles that cannot be placed

$$(2.13)$$

$$(x_R, y_R)$$

$$\begin{pmatrix} x_N \\ y_N \end{pmatrix} = \begin{pmatrix} \cos\theta & -\sin\theta \\ \sin\theta & \cos\theta \end{pmatrix} \begin{pmatrix} x_R \\ y_R \end{pmatrix} \quad (2.13)$$

Fig. 2.25.

가 가

'0'
'0'

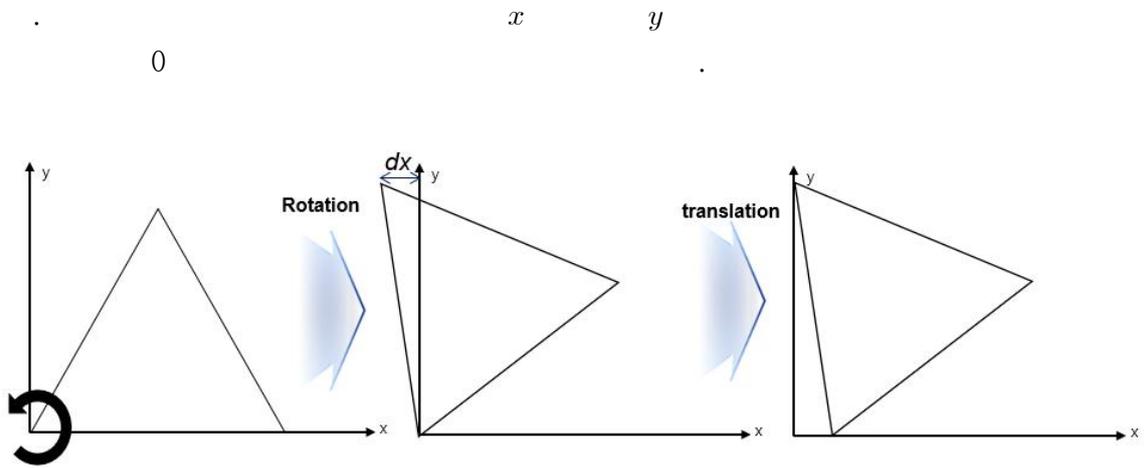


Fig. 2.25. Rotation of the piece

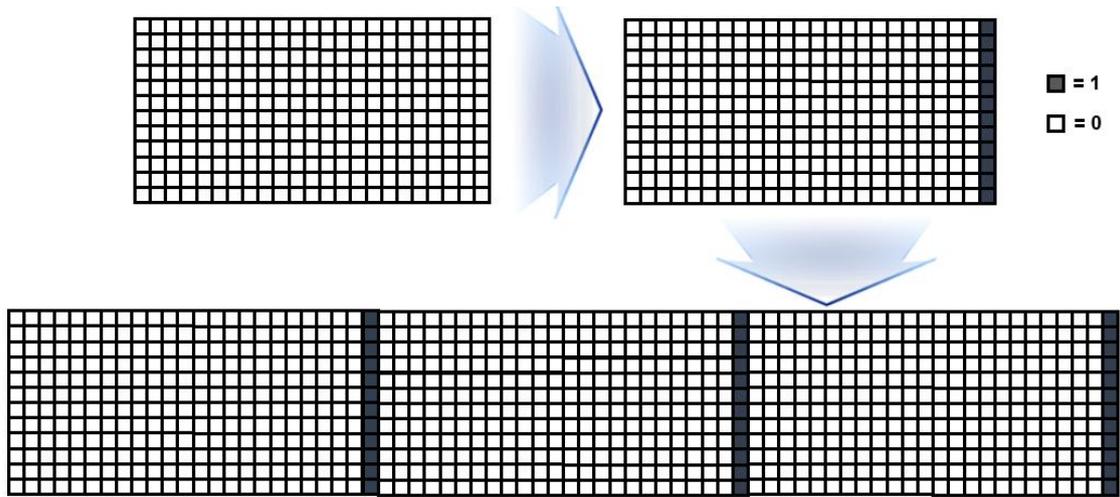


Fig. 3.2. Representation of multiplate grids

Fig. 3.2. 가 . 가 , 가 '1' 가 .

3.3.

3.3.1.

(GA, Genetic Algorithm)

[29]

(Population) 가

(Population)

(Gene)

(Chromosome)

Fig. 3.3.

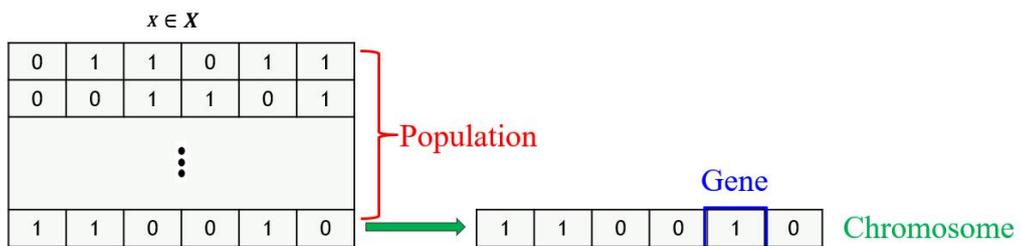


Fig. 3.3. The components of a poluation

(Mutation) (Selection), (Crossover), 가

Fig. 3.4

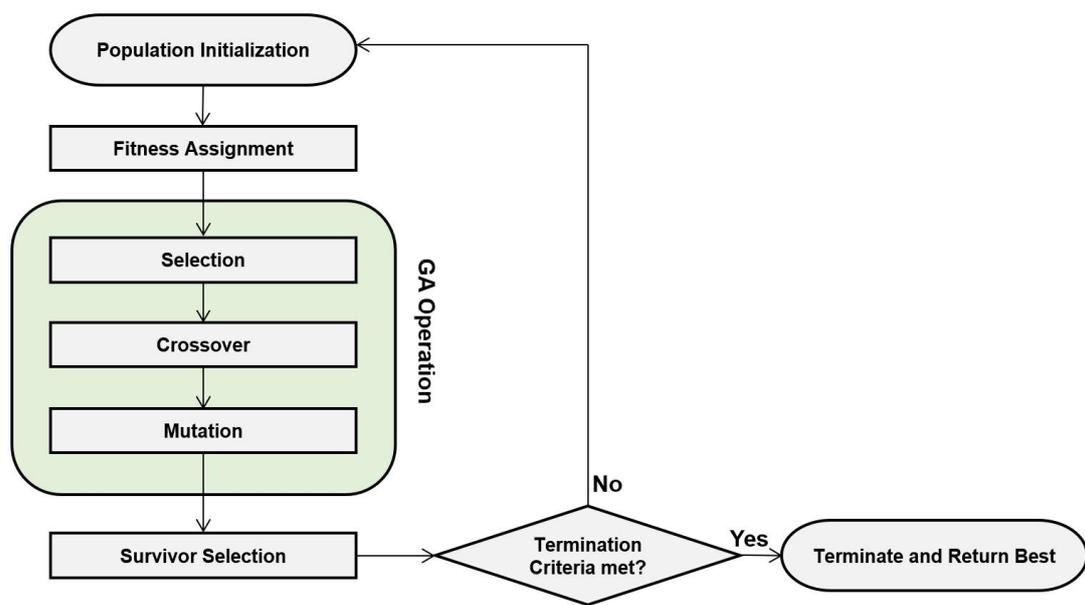


Fig. 3.4. Basic steps of genetic algorithm

Table. 3.1. [29]

가

Table. 3.1. The procedure of a general GA[30]

Algorithm. Genetic Algorithm

Step1: Set $t=1$. Randomly make N solutions to form the chromosome, P_1 . Evaluate the fitness of solution in P_1 .

Step2: Fitness assignment: Evaluate and obtain a fitness value to each solution $x \in Q_t$ using its objective function value.

Step3: Selection: Select N solutions from Q_t based on their fitness and copy them to P_{t+1}

Step4: Crossover: Generate an offspring chromosomes Q_t as follows:

4.1 Select several solutions x from P_t based on the fitness values

4.2 Using a crossover operator, generate offspring and add them to Q_t

Step5: Mutation: Mutate each solution $x \in Q_t$ with a predefined probability

Step6: If the object function is converged, terminate the search and return to the current best solution, else, set $t=t+1$ go to *Step2:*

. Kim[31]

가

가

가

3.2.1.1

3.3.1.1. Fitness function

가

Fitness function

가

가

(3.1)

$$fitness = \sum_{i=1}^{i = NumberOfPlates} i^2 \cdot f_i \quad (3.1)$$

(3.1) i f_i i Fig. 3.5. 4 가 Fig.
 3.5. 가 , 가
 f_1 , f_2 가 . $fitness$
 i^2 가
 Fig. 3.6. Fig. 3.5. 가
 i^2 Fig. 3.5. Fig. 3.6.
 Fig. 3.6.

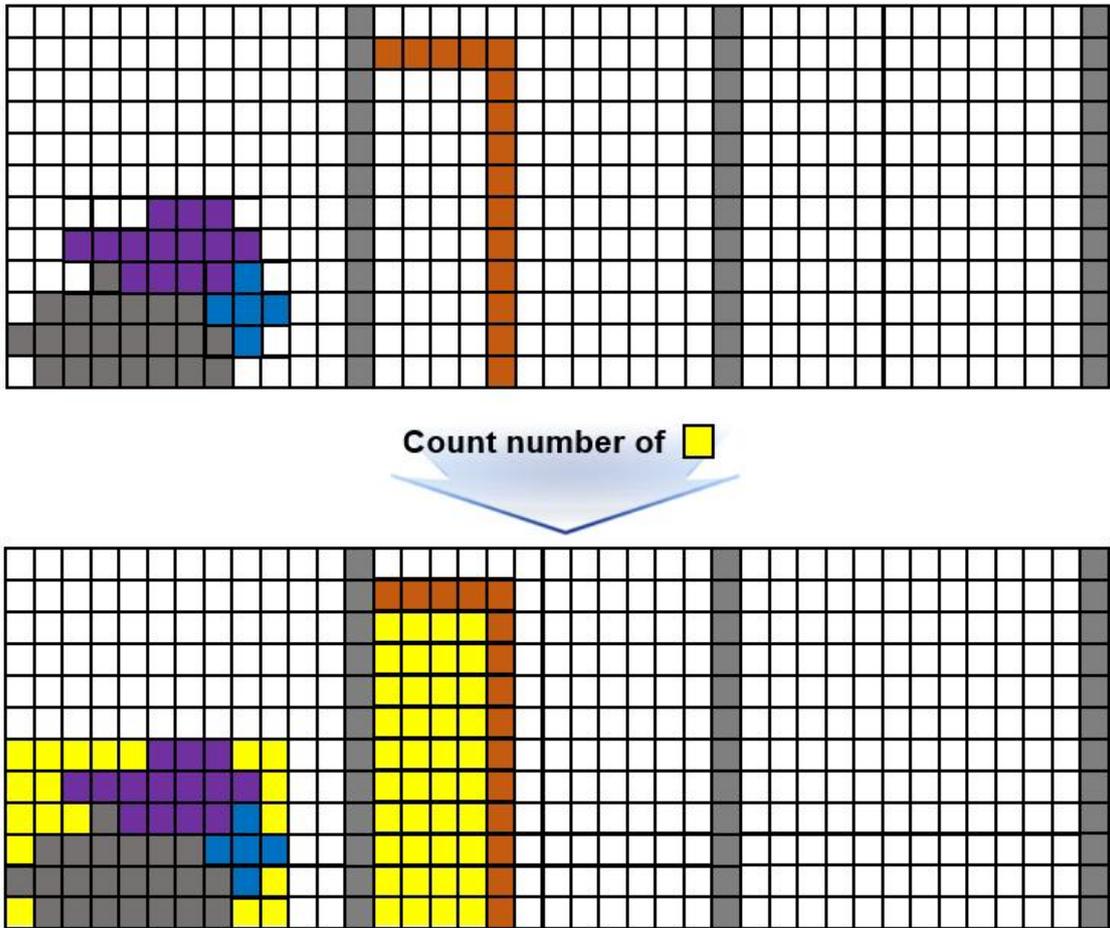


Fig. 3.5. Case1 : Calculation of the fitness function

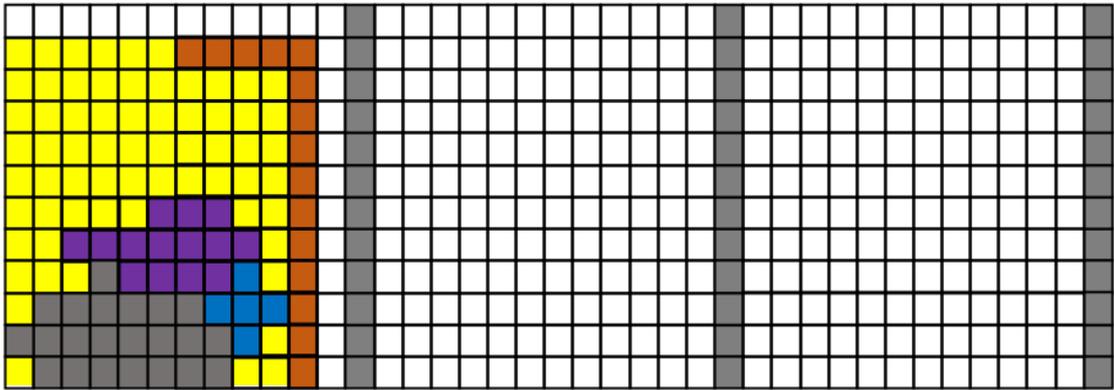
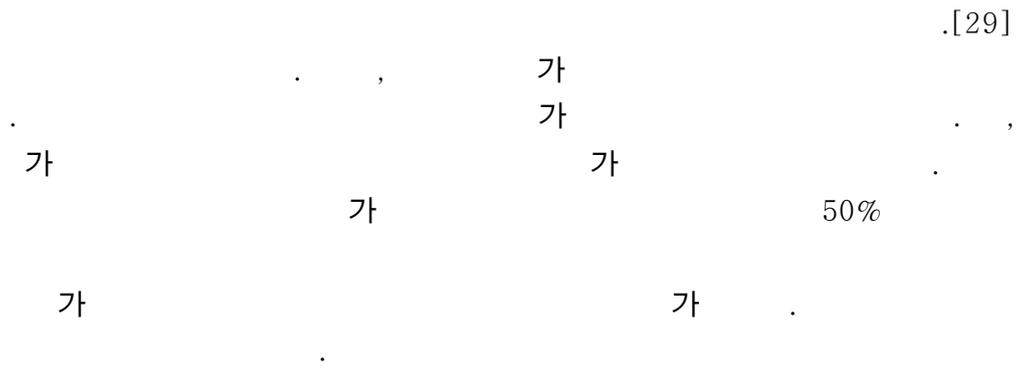
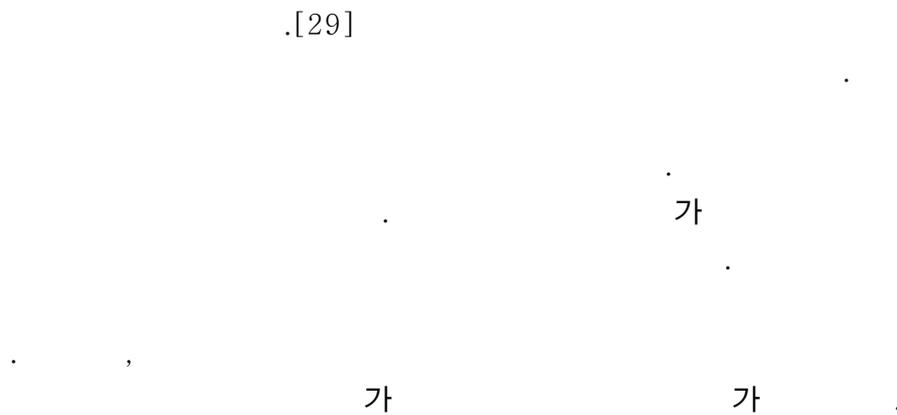


Fig. 3.6. Case2 : Calculation of the fitness function

3.3.1.2. Selection



3.3.1.3. Crossover



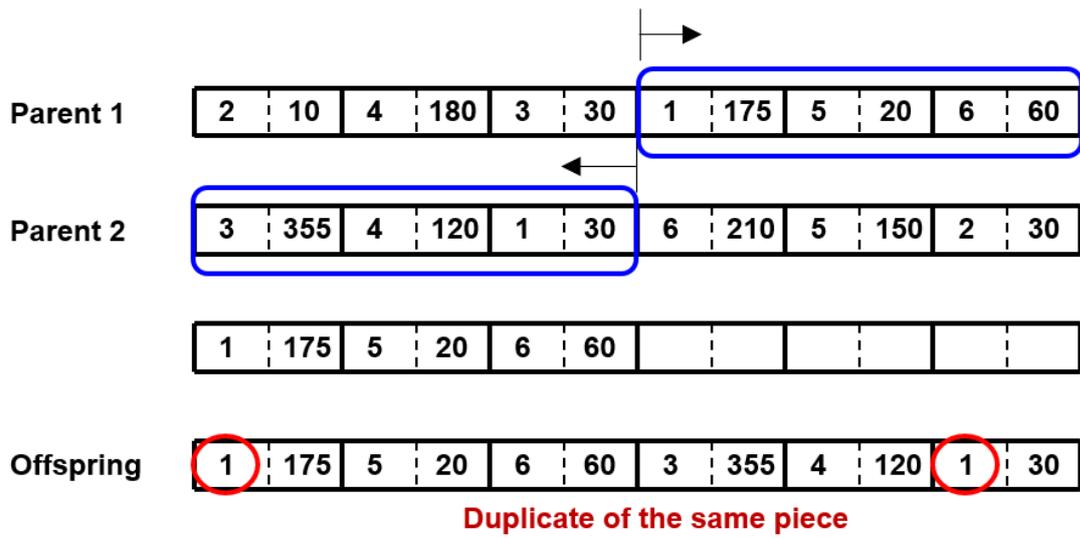


Fig. 3.7. Duplication of genes

Fig. 3.7.

가

. (Fig. 3.8.)

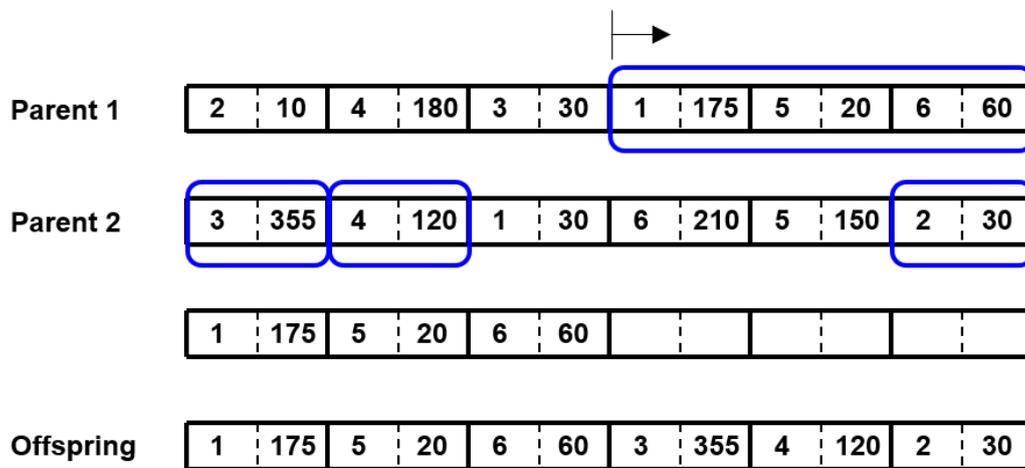


Fig. 3.8. Elimination of gene duplication

3.3.1.4. Mutation

가

가

가

가

. (Fig. 3.9.)

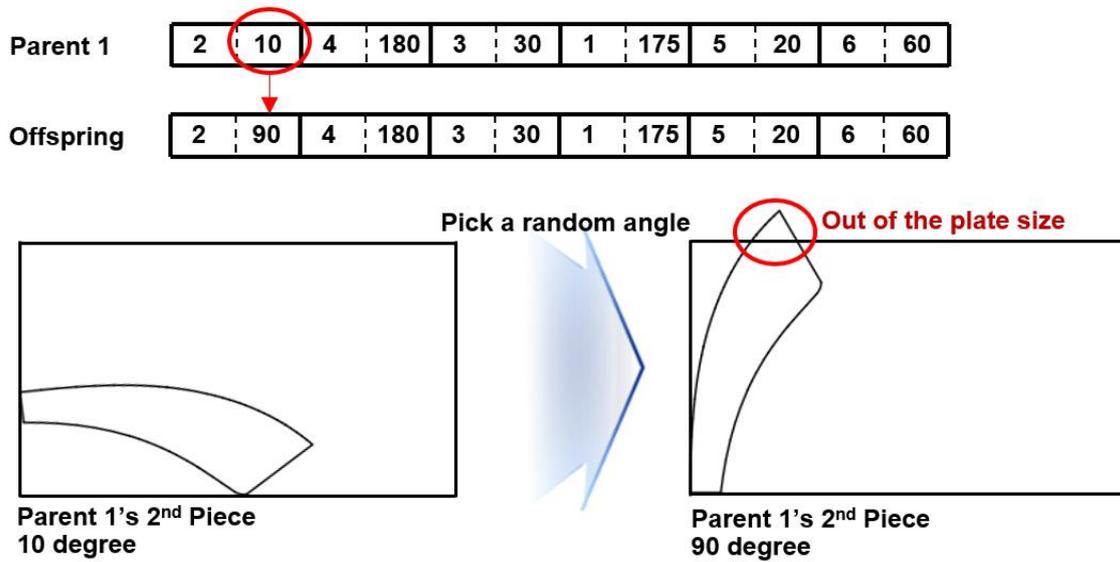


Fig. 3.9. Increased piece vertical size due to rotation of angle

가

가

.(Fig. 3.10.)

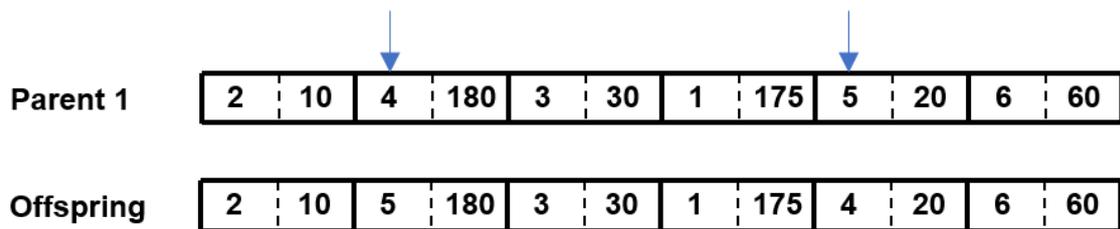


Fig. 3.10. Mutation operation on layout order

3.4.
3.4.1.

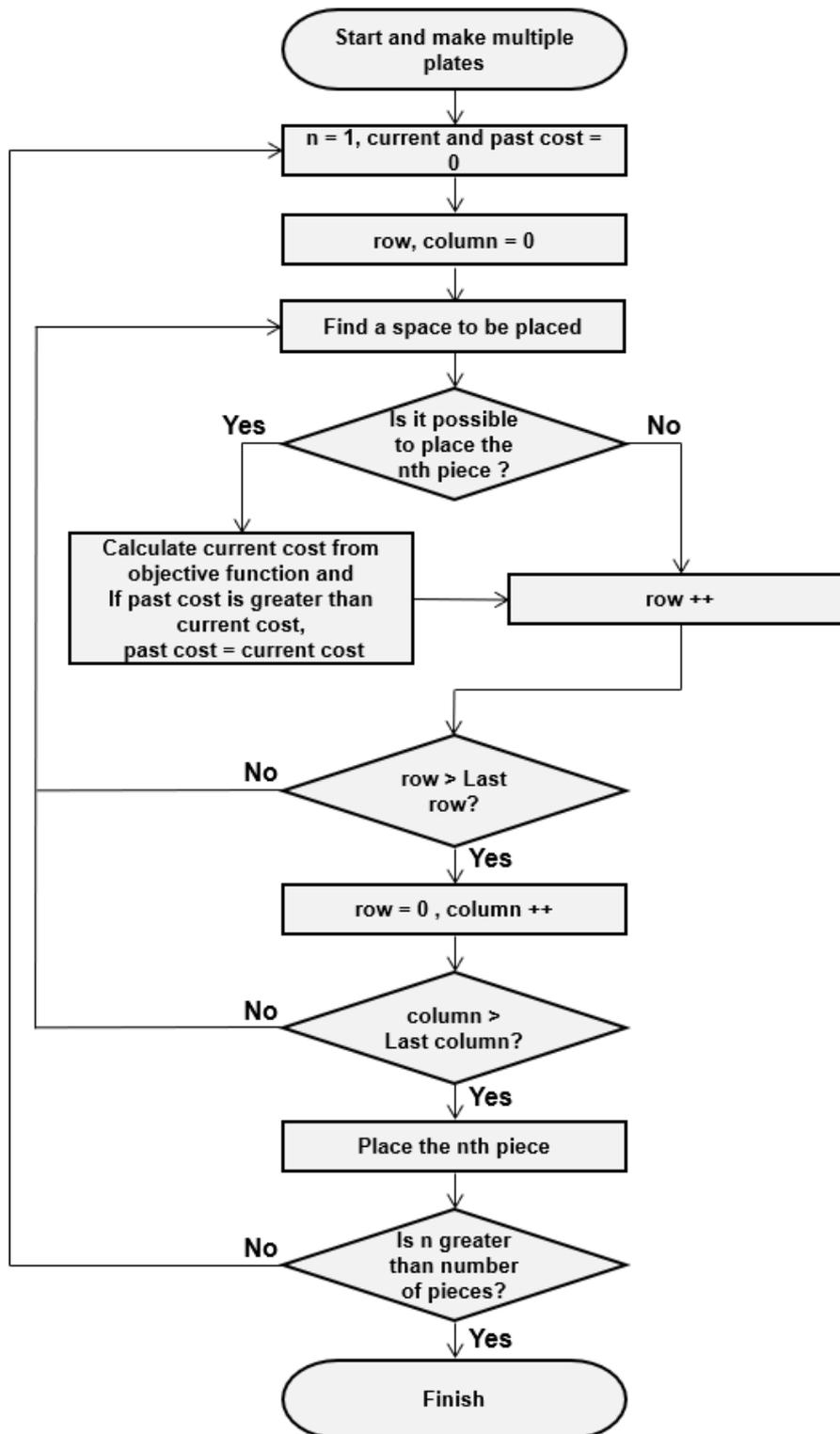


Fig. 3.11. Layout algorithm flow chart

Kang[10]

가 '1' '1' '1'
 .(Fig. 3.12.)

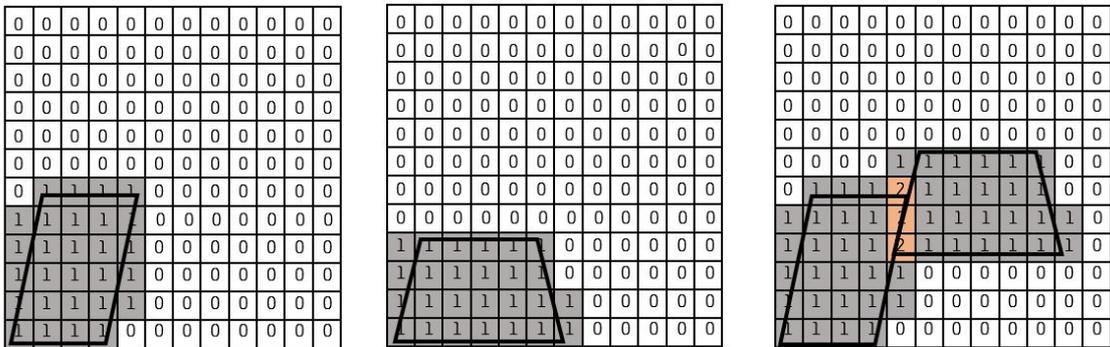


Fig. 3.12. Overlap detection of two pieces

Fig. 3.13.

가

Case1

가

Case2

가

가

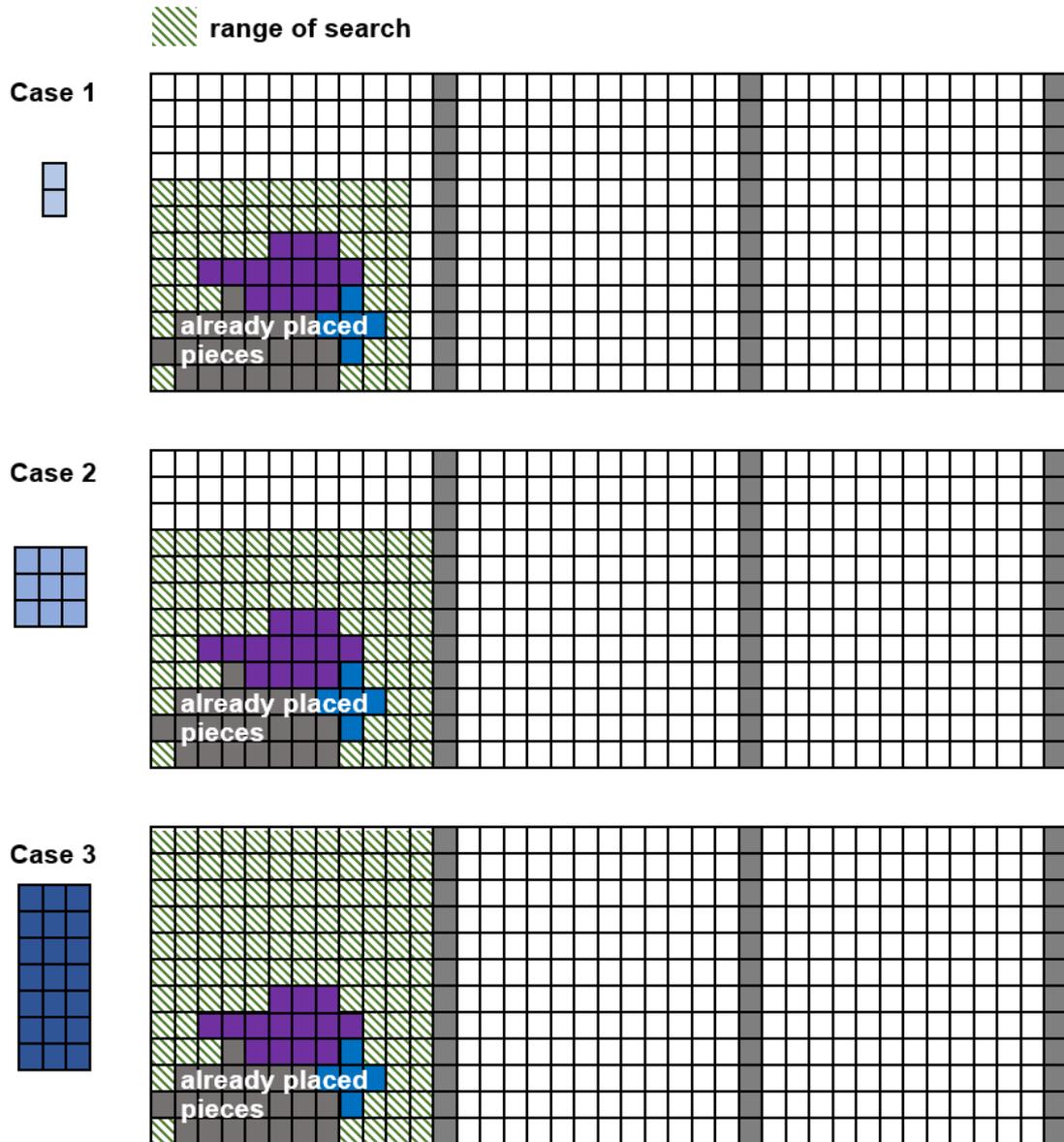


Fig. 3.13. Search Range of pieces to be placed

3.4.2.

가 (Objective functions)
 (Cost) . 가 . Kang[10]

$$Min(F) = f_x + f_y + f_{xy} \quad (3.2)$$

f_x, f_y, f_{xy} .

f_x 가 f_y 가 f_{xy} 가

(Fig. 3.14.)

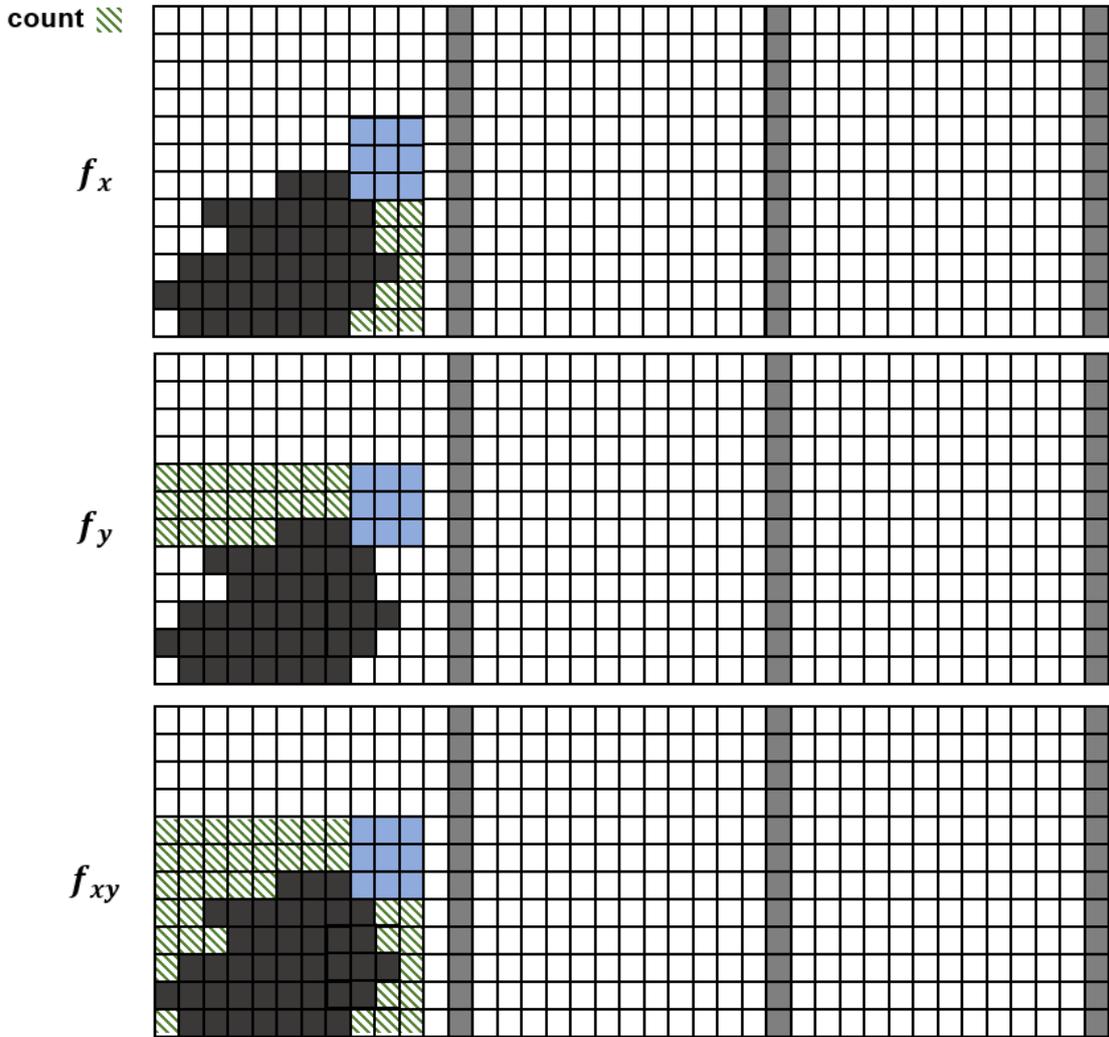


Fig. 3.14. Calculation of the objective function f_x , f_y , and f_{xy}

Lee[32] (Scrap ratio) 가

$$f_y, f_{xy}, f_y, f_{xy}$$

(3.3)

$$Min(F) = \sum_{i=1}^{Number\ of\ Plates} (f_y)_i + (f_{xy})_i \quad (3.3)$$

3.5.

: 1200mm, 가 : 2400mm 25mm
 50mm 가
 0°, 5°, 10°, 15°, 20°, 30°, 60°, 90°, 120°, 150°, 180°, 210°, 240°, 270°, 300°, 330°, 340°, 345°, 350°, 355°
 20° 5°
 30° . Fig. 3.15. 8
 post script
 Intel(R) Core(TM) i9-10900 CPU @ 2.80GHz
 16.0GB RAM .

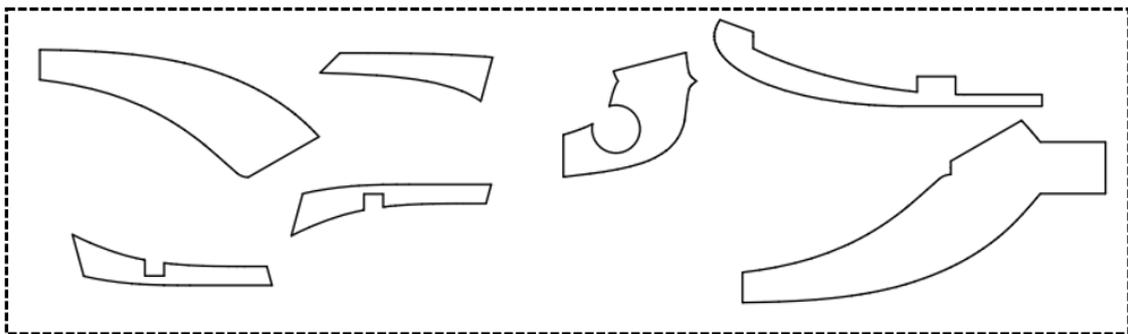


Fig. 3.15. Pieces of the Model ship

5가

가 5가
 (3.1) . Fig. 3.16 Fig. 3.17 25mm
 . Fig. 3.16.

가 3.19381 .

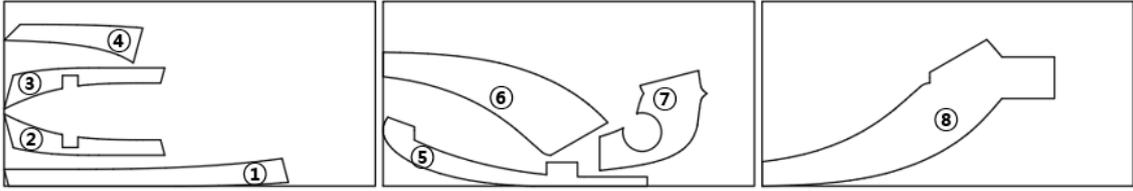


Fig. 3.16. Arrangement in order of aspect ratio

Fig. 3.17.
1.62284 .

가

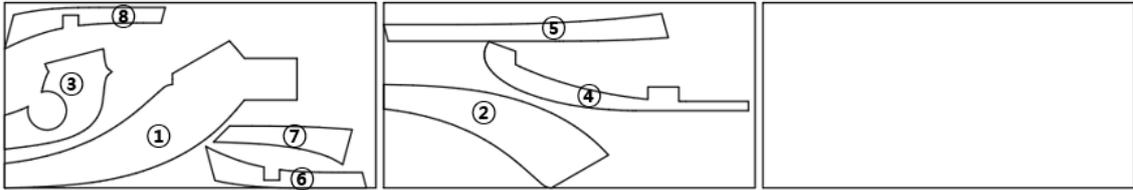


Fig. 3.17. Arrangement in order of area

Fig. 3.16. Fig. 3.17

Fig. 3.18.

f_{xy}

가

1.27155 .

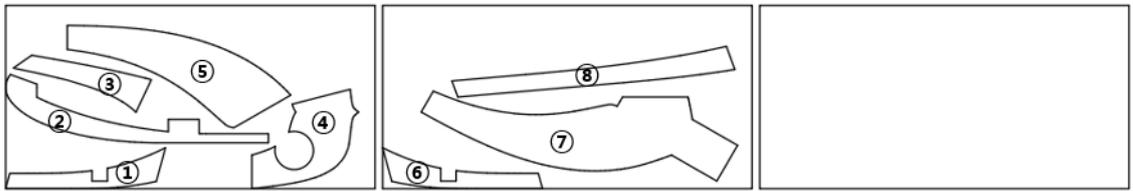


Fig. 3.18. Case 1 of Arrangement using genetic algorithm

Fig. 3.19. 가

Fig. 3.18 .

가

1.17361 .

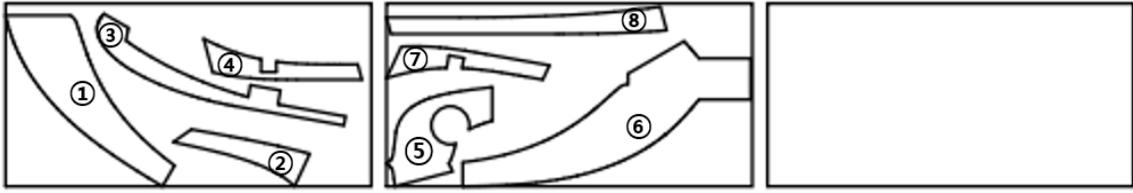


Fig. 3.19. Case 1 of Arrangement using genetic algorithm when the grid size is 50mm

Fig. 3.18. Fig. 3.19. 가 . 가
 가 가 가 가 .
 가 가

Fig. 3.20.

f_{xy} . 가
 1.10652 .

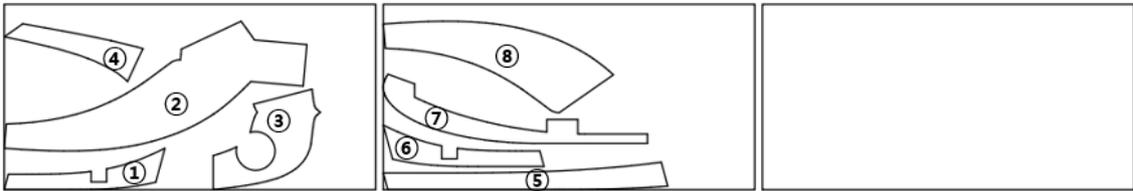


Fig. 3.20. Case 2 of Arrangement using genetic algorithm when the grid size is 25mm

Fig. 3.21.

Fig. 3.20 . 가 1.17361 .

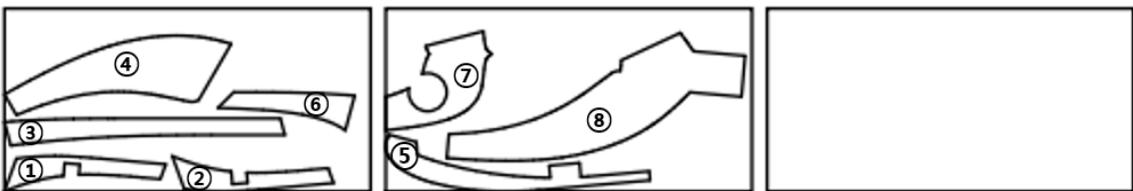


Fig. 3.21. Case 2 of Arrangement using genetic algorithm when the grid size is 50mm

Fig. 3.21. 5 가 가 6 가
 Fig. 3.18. Fig. 3.19 가 Fig. 3.20. Fig. 3.21. 가
 Case 1 Case 2 가
 가

Fig. 3.22.

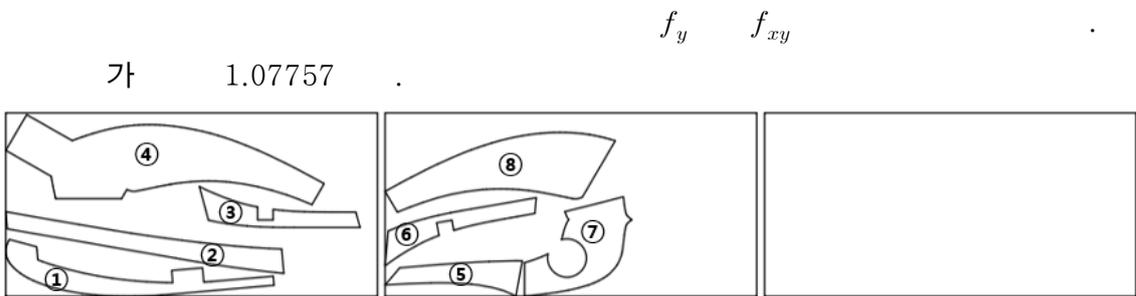


Fig. 3.22. Case 3 of Arrangement using genetic algorithm when the grid size is 25mm

Fig. 3.23.

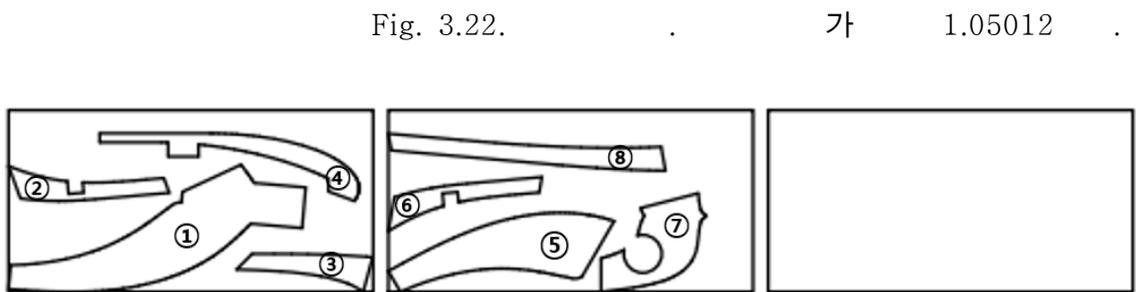


Fig. 3.23. Case 3 of Arrangement using genetic algorithm when the grid size is 25mm

Fig. 3.22 Fig. 3.23 , 25mm

Fig. 3.24
 (b)가 (a) 가 (b)가

(a), (b)
가

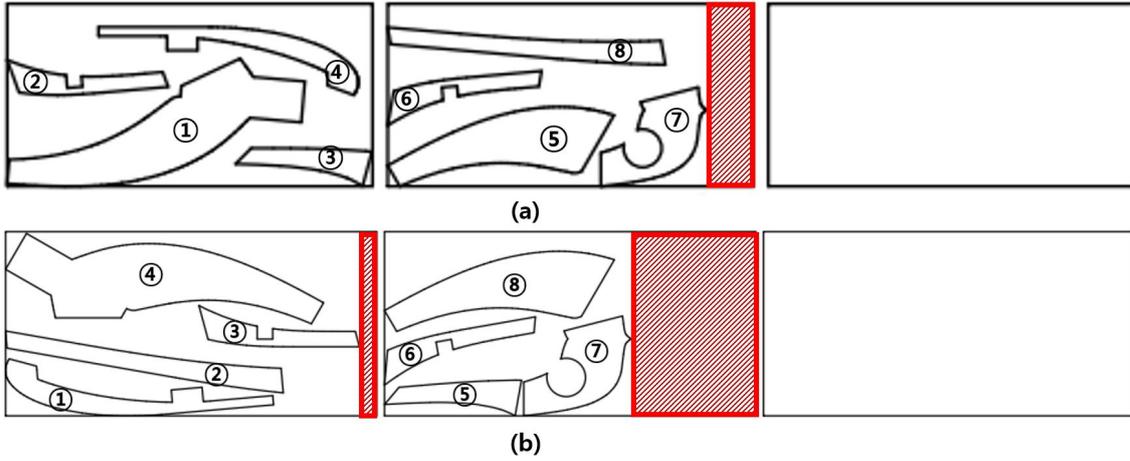


Fig. 3.24. Comparison of reusability when grid sizes are different

(Fig. 3.16.),
(Fig. 3.17.)

(Fig. 3.18.)(Fig. 3.19.)(Fig. 3.20.)

가

Case1(Fig. 3.18., Fig. 3.19.) ,

f_{xy}

. Case2(Fig. 3.20., Fig. 3.21.)

3.22., Fig. 3.23) Case1, Case2

f_y f_{xy}

. Case3(Fig.

가

1.07757 1.05012 .

4

(Polyline)

G-code

G-code

. 4.1

4.1 G-code

Table. 4.1. G-code list

G-code	Group	Property	Function
G00	01	modal	Rapid postioning
G01			Linear interpolation
G02			Circular interpolation CW
G03			Circular interpolation CCW

G-code

G-code

. Table. 4.1.

4가 G

G00

. G01

가

G02

G03

가

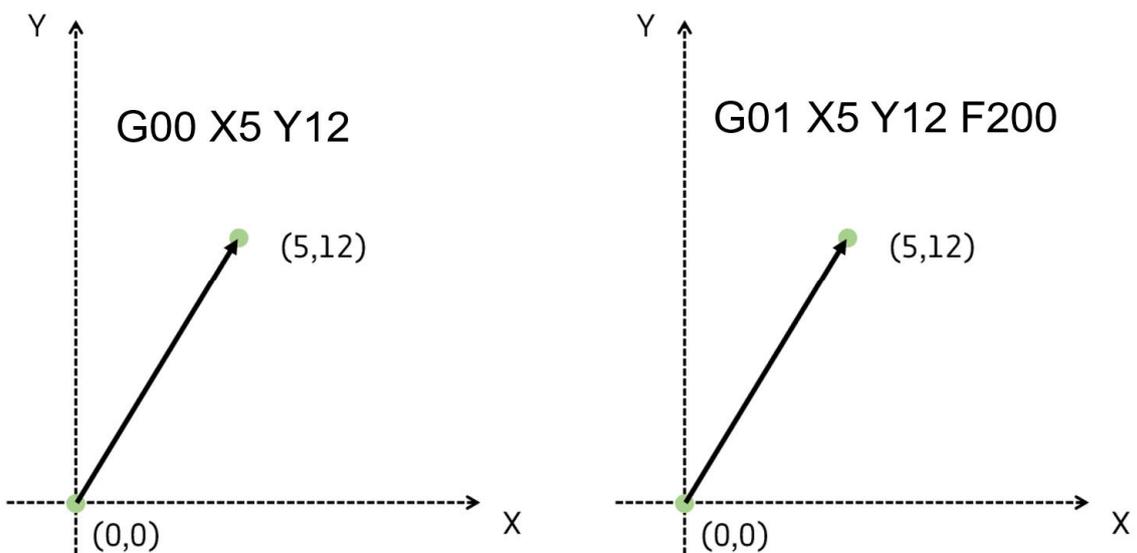


Fig. 4.1. Example for G00 and G01

Fig. 4.1. G00, G01
 G00 X Y G01
 F200 가

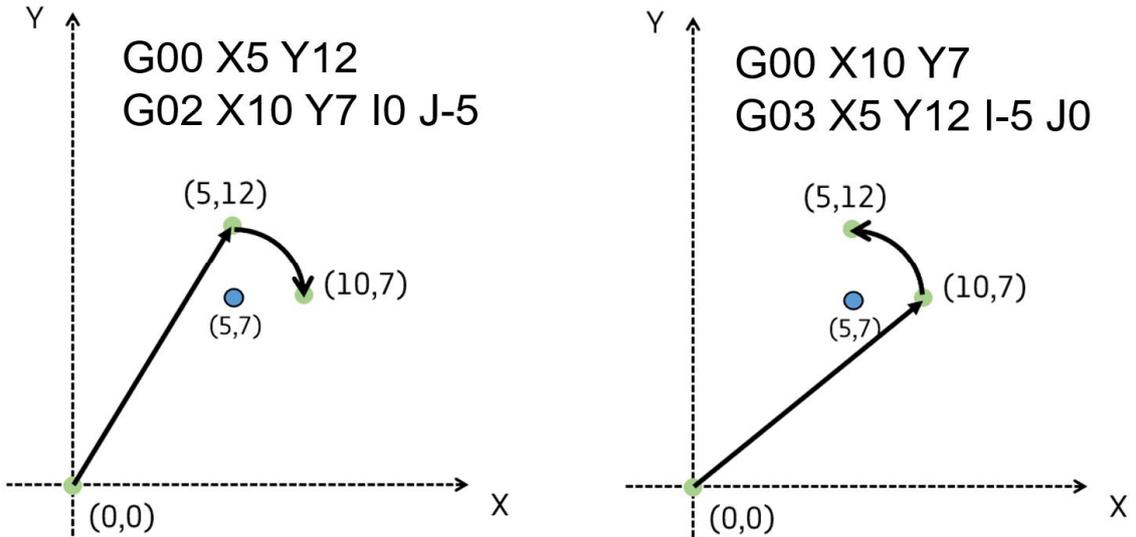


Fig. 4.2. Example for G02 and G03

Fig. 4.2. G-code
 가 가 (5,12)
 (5,7) (10,7)
 Fig. 4.2.
 G-code . I J
 가 G-code

4.2

4.2.1

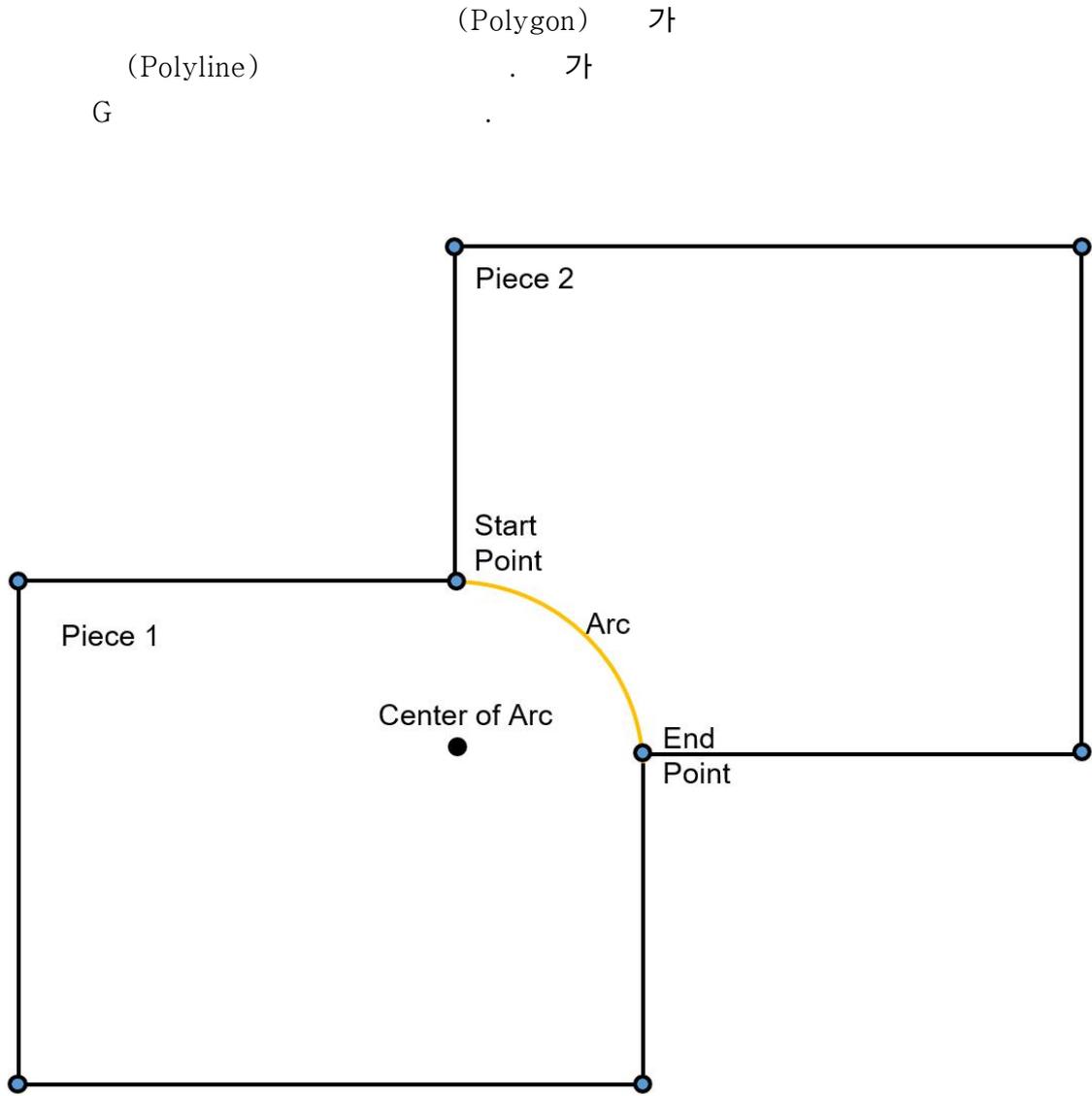


Fig. 4.3. Examples of reasons for judging convexity

Fig. 4.3. Arc ,

. Piece 1 Arc가

가 , Arc G02

. Piece 2 Arc가

가 , G03

. G02 G03

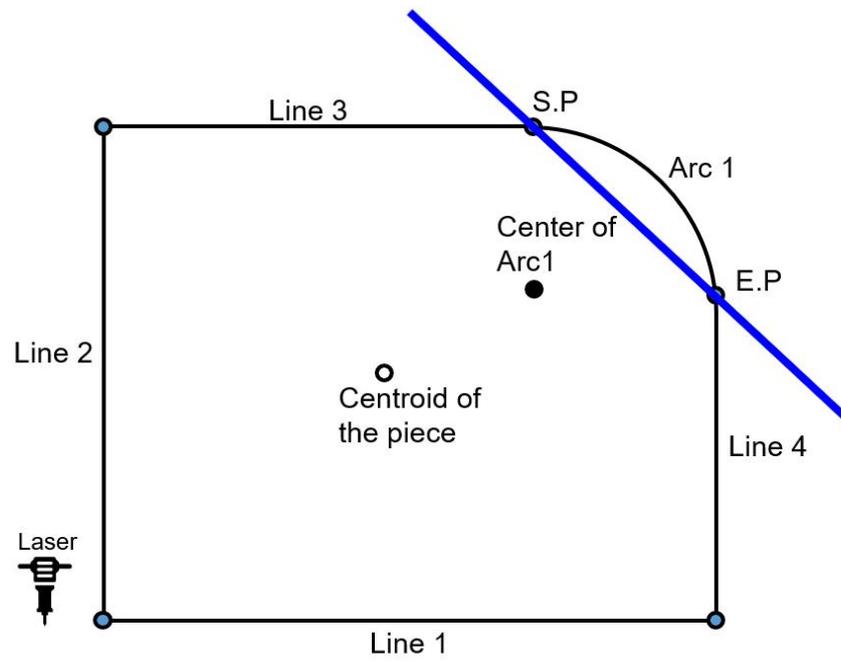


Fig. 4.4. Example when the arc of the piece is convex

Fig. 4.4.

가

x,y

'Arc1'

'Arc1'

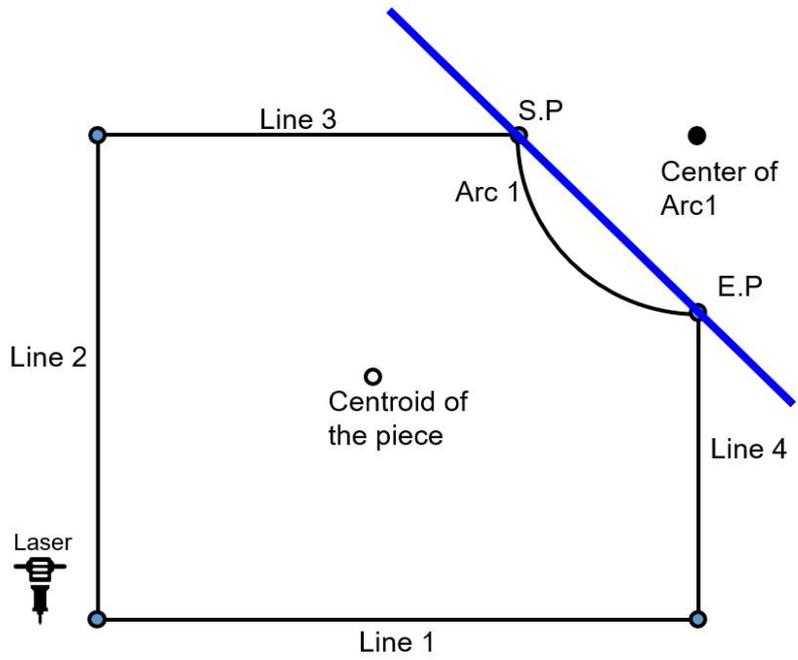


Fig. 4.5. Example when the arc of the piece is concave

Fig. 4.5.

'Arc1'

'Arc1'

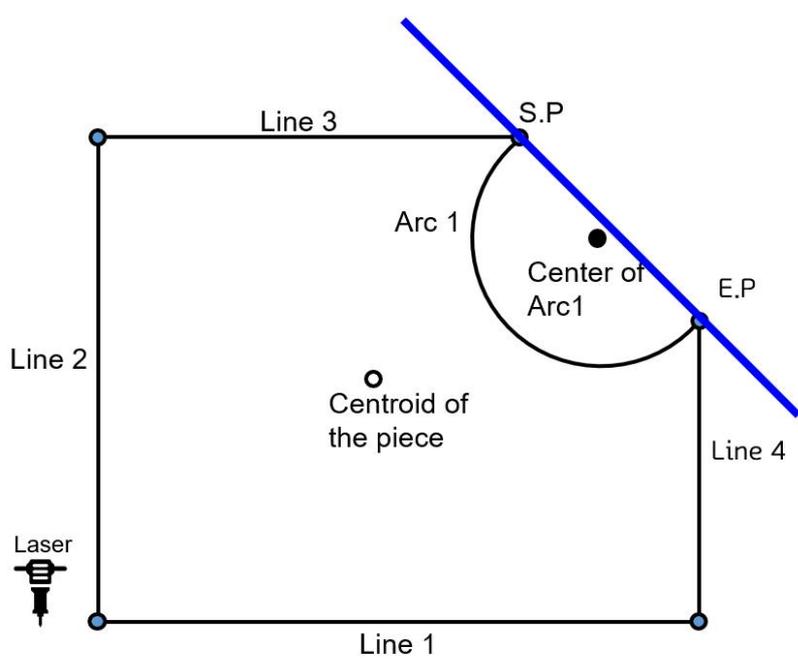


Fig. 4.6. Exception Case example when the arc of the piece is concave

Fig. 4.5.

Fig. 4.6.

가 180°

Fig. 4.7.

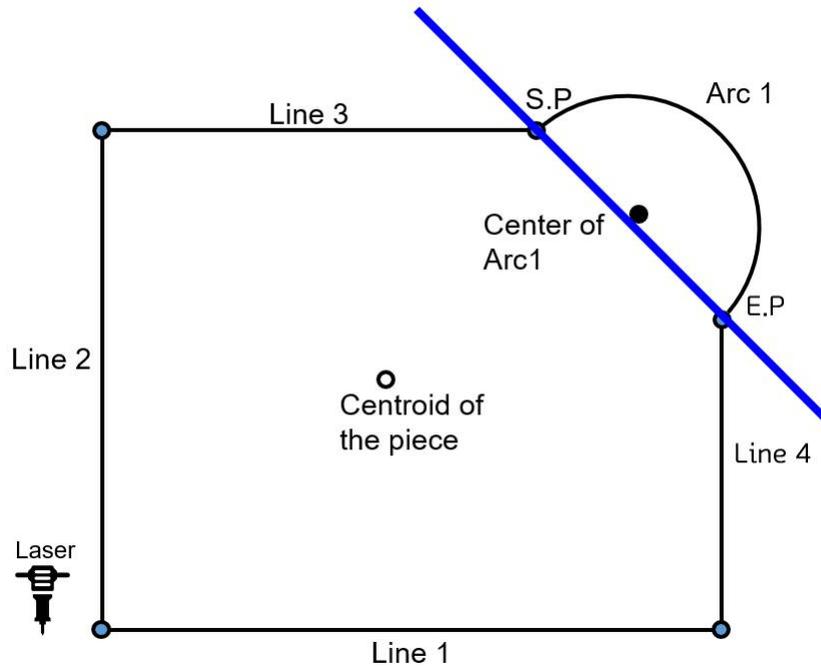


Fig. 4.7. Exception case example when the arc of the piece is convex

Table. 4.2.

Table. 4.2. Determination of convexity according to arc angle

degree	Sign	Convex or Concave
less than 180°	Different Sign	Concave
	Same Sign	Convex
over 180°	Same Sign	Convex
	Different Sign	Concave

4.2.2

(GA)

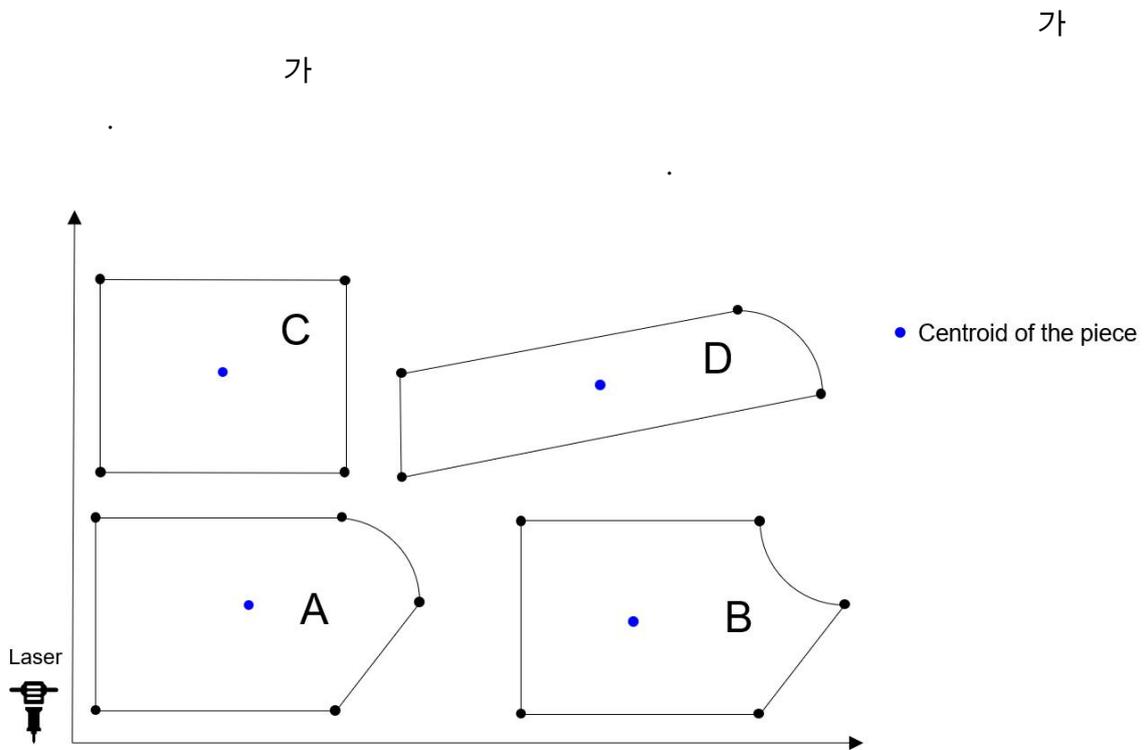


Fig. 4.8. Example of arrangement result including arc and line

Fig. 4.8.

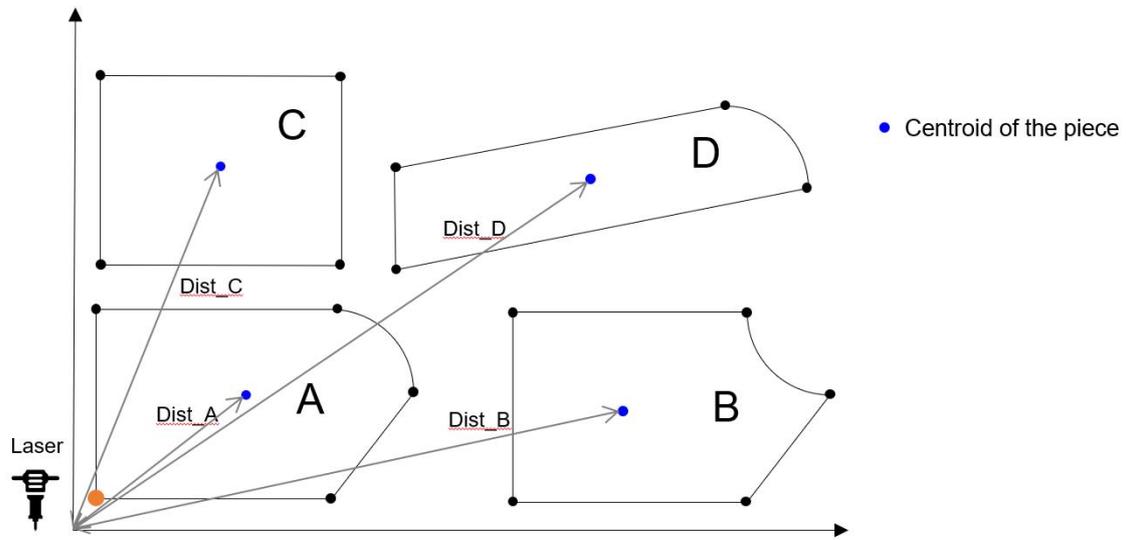


Fig. 4.9. Example of how to select the first piece

가 . Fig. 4.10. A가 . A가
가 가 가

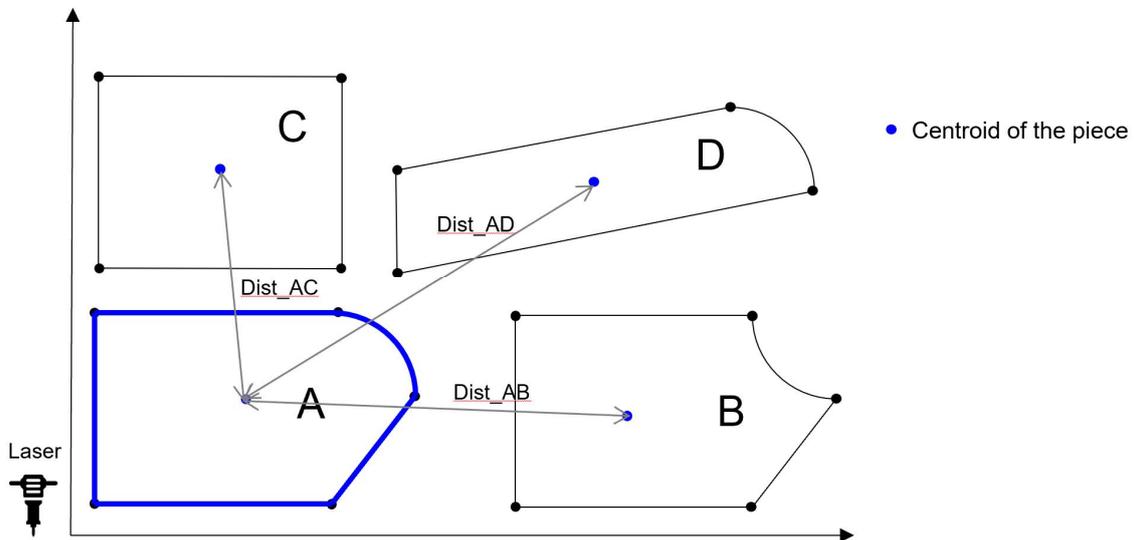


Fig. 4.10. Example of how to select the second piece

A , A
가 가
C .(Fig. 4.11)

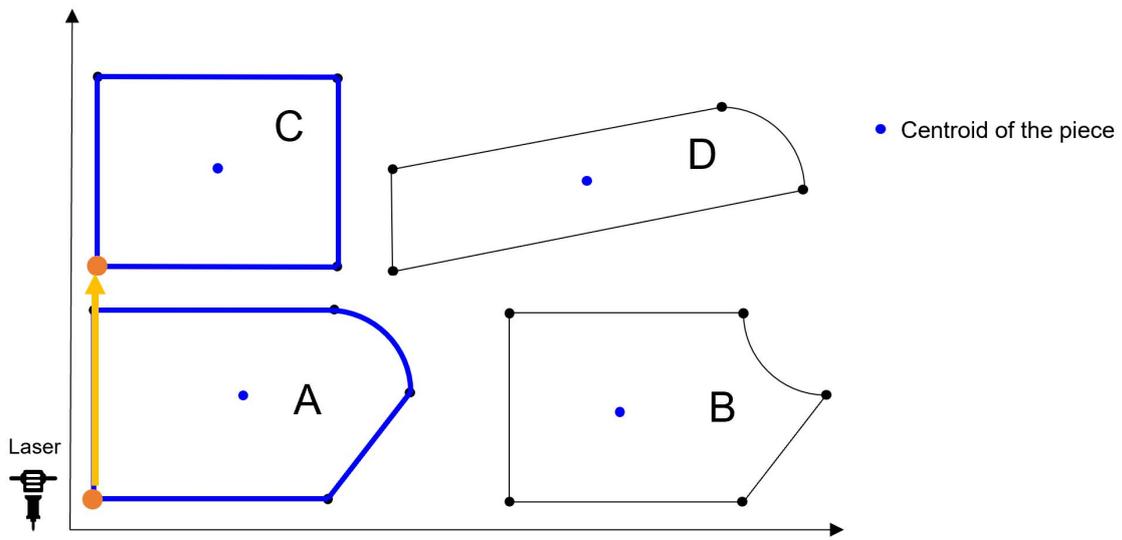


Fig. 4.11. method for calculating the shortest path between the first piece and the second piece

가
가 가
가 . Fig. 4.11.
G-code G00

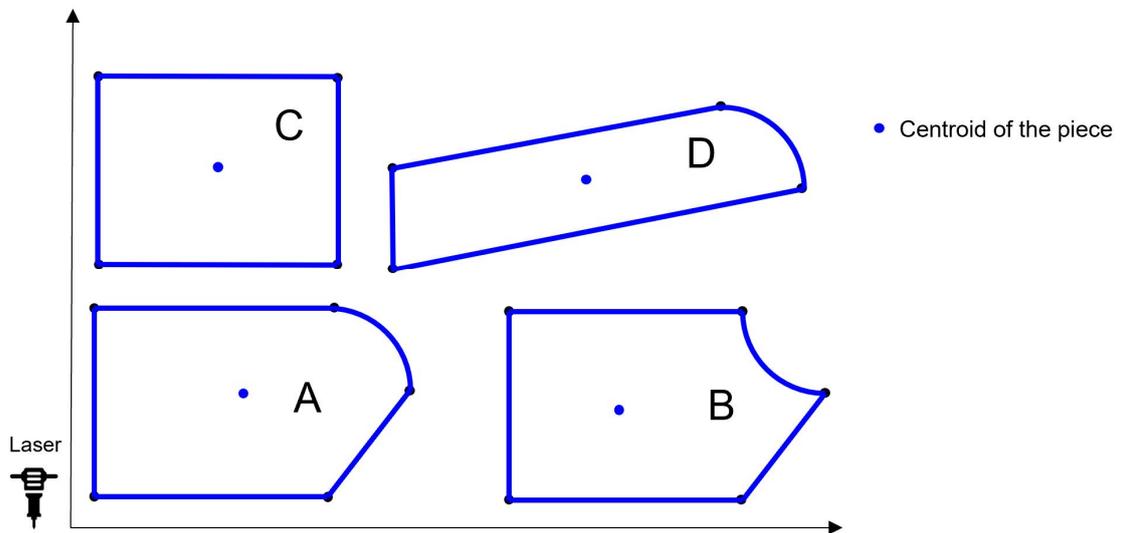


Fig. 4.12. Result of piece cutting completion

Polyline A,B,C,D . (Fig. 4.12.)

4.2.3

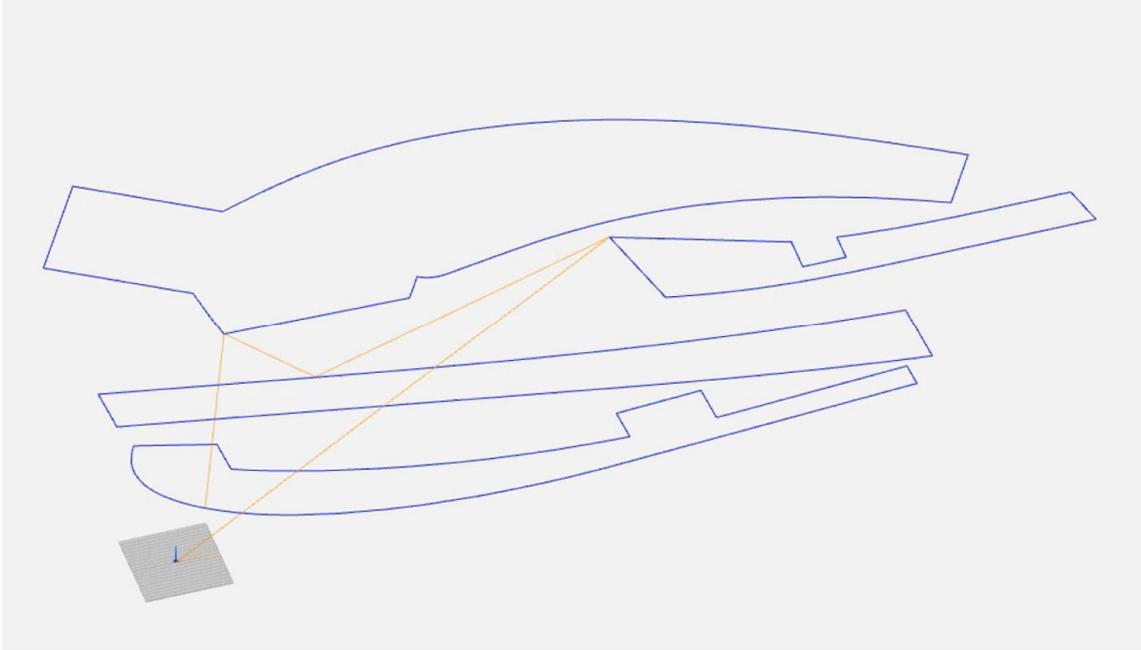


Fig. 4.13. Verification of cutting path generation algorithm of model ship pieces

가

.(Fig. 4.13.)

가

가

가

5

NC

가
가
'1'
가
가 3.19381 3
가 1.62284 2
25mm 50mm
 f_{xy} 2가
가
1.27155 1.17361 2
가 1.10652 1.07411 2
가 25mm
가
가
 f_{xy}, f_y
가 1.07757 1.5012 2
3가 가
waterline
가
가

가 가

가 가

가 가

NC

가

- [1] Guo, Baosu, et al. 2020. "Automatic layout of 2D free-form shapes based on geometric similarity feature searching and fuzzy matching." *Journal of Manufacturing Systems* 56 : 37–49.
- [2] Adamowicz, M., & Albano, A. 1976. A solution of the rectangular cutting-stock problem. *IEEE Transactions on Systems, Man, and Cybernetics*, (4), 302–310.
- [3] Dori, D., & Ben-Bassat, M. 1984. Efficient nesting of congruent convex figures. *Communications of the ACM*, 27(3), 228–235.
- [4] Adamowicz, M., & Albano, A. 1976. Nesting two-dimensional shapes in rectangular modules. *Computer-Aided Design*, 8(1), 27–33.
- [5] Albano, A. 1977. A method to improve two-dimensional layout. *Computer-Aided Design*, 9(1), 48–52.
- [6] A. R. Babu and N. R. Babu, 2001. "A generic approach for nesting of 2-D parts in 2-D sheets using genetic and heuristic algorithms," *Computer-Aided Design*, vol. 33, pp. 879–891,
- [7]Konopasek, M. 1981. Mathematical treatments of some apparel marking and cutting problems. US Department of Commerce Report, 99(26), 90857–10. problems," US Department of Commerce Report, vol. 99, pp. 90857–10, 1981.
- [8]Y. Stoyan, G. Scheithauer, N. Gil, and T. Romanova, 2004. Phi-functions for complex 2D-objects, *Quarterly Journal of the Belgian, French and Italian Operations Research Societies*, vol. 2, pp. 69–84,
- [9] . 2000. .
- [10] . 1998. .
- [11] Kim, Y., Gotoh, K. and Toyosada, M., 2003. "Automatic twodimensional layout using a rule-based heuristic algorithm",*Journal of Marine Science and Technology*,Vol.8, pp. 37–46,
- [12]Weng, W.C. and Kuo, H.C. 2011. "Irregular Stock Cutting System Based on AutoCAD", *Advances in Engineering Software*, Vol 42, pp 634–643
- [13]Liu Q, Zeng J, Zhang H, Wei L . 2020. A heuristic for the twodimensional irregular bin packing problem with limited rotations. In: Fujita H, Fournier-Viger P, Ali M, Sasaki J (eds.) *Trends in artificial intelligence theory and applications. Artificial intelligence practices*, pp 268–279. Springer
- [14] Han, G.C. and Na S.J., 1996. Two-stage approach for nesting in

two-dimensional cutting problems using neural network and simulated annealing
Proceedings of the Institution of Mechanical Engineers, Journal of Engineering
manufacture, Vol.210, pp.509–519,

[15]Luo Q, Rao Y, Peng D. 2022. Ga and gwo algorithm for the special bin
packing problem encountered in field of aircraft arrangement. Applied Soft
Comput, 114, 108060.

[16]Sheen, D. M. 2012. Nesting expert system using heuristic search. Journal
of Ocean Engineering and Technology, 26(4), 8–14.

[17] , & . 2000.
 , 37(3), 90–98.

[18] , & . 2009.
 , 23(6), 67–70.

[19]Al-Sahib, N. K. A., & Abdulrazzaq, H. F. 2014. Tool path optimization of
drilling sequence in CNC machine using genetic algorithm. Constraints (2a), 2,
2b.

[20]Lee, M. K., & Kwon, K. B. 2006. Cutting path optimization in CNC cutting
processes using a two-step genetic algorithm. International Journal of
Production Research, 44(24), 5307–5326.

[21]Hajad, M., Tangwarodomnukun, V., Jaturanonda, C., & Dumkum, C. 2019.
Laser cutting path optimization using simulated annealing with an adaptive large
neighborhood search. The International Journal of Advanced Manufacturing
Technology, 103, 781–792.

[22] . 1989.
 ,
 , pp3–15.

[23]Mander, U. and Israni, S., 1984, “Piece Point Minimization and Optimal
Torch Path Determination in Flame Cutting,” Journal of Manufacturing Systems,
Vol.3, No. 1, pp.81–89,

[24] , , 1993, “ NC
 ”,
 , 17(5), pp. 1183–1192,

[25] , & . (1996).
 , 20(6), 1827–1835.

[26]Silvela, Jaime, and Javier Portillo., 2001, "Breadth-first search and its
application to image processing problems.", *IEEE Transactions on Image
Processing* 10.8 , 1194–1199.

[27] E. K. Burke, R. S. Hellier, G. Kendall, and G. Whitwell, 2007. Complete
and robust no-fit polygon generation for the irregular stock cutting problem,
European Journal of Operational Research, vol. 179, pp. 27–49,

[28] Bresenham, J.E., 1965. Algorithm for Computer Control of a Digital

Plotter. IBM System Journal, 4(1), 25–30

[29] Goldberg D.E., 1989. “Genetic Algorithms in Search, Optimization and Machine Learning (1st. ed.)”, Addison–Wesley Longman Publishing Co., Inc., USA.

[30] Konak A., Coit D.W., Smith A.E., 2006. “Multi–objective optimization using genetic algorithms: A tutorial”, Reliability Engineering & System Safety, Vol. 91, Issue 9, Pages 992–1007, ISSN 0951–8320,

[31] Kim, D. S., & Lee, C. S. 2009. Determination of an optimal sequence for nesting with heuristic algorithm. In CAD/CAM Conference.

[32] Lee, H.B., & Ruy, W.S. 2013. Determination of Nesting Algorithm Fitness Function through Various Numerical Experiments. Journal of Ocean Engineering and Technology, 27(5), 28–35.